

Identification and transcriptomic profiling of salinity stress response genes in colored wheat mutant

Min Jeong Hong¹, Chan Seop Ko¹, Jin-Baek Kim¹, Dae Yeon Kim^{Corresp. 2}

¹ Advanced Radiation Technology Institute, Korea Atomic Energy Research institute, Jeongeup, Jeollabuk-do, Korea

² Plant Resources, Kongju National University, Yesan-eup, Chungnam, South Korea

Corresponding Author: Dae Yeon Kim
Email address: dykim@kongju.ac.kr

Background. Salinity is a major abiotic stress that prevents normal plant growth and development, ultimately reducing crop productivity. This study investigated the effects of salinity stress on two wheat lines: PL1 (wild type) and PL6 (mutant line generated through gamma irradiation of PL1).

Results. The salinity treatment was carried out with a solution consisting of a total volume of 200 mL containing 150 mM NaCl. Salinity stress negatively impacted germination and plant growth in both lines, but PL6 exhibited higher tolerance. PL6 showed lower Na⁺ accumulation and higher K⁺ levels, indicating better ion homeostasis. Genome-wide transcriptomic analysis revealed distinct gene expression patterns between PL1 and PL6 under salt stress, resulting in notable phenotypic differences. Gene ontology analysis revealed positive correlations between salt stress and defense response, glutathione metabolism, peroxidase activity, and reactive oxygen species metabolic processes, highlighting the importance of antioxidant activities in salt tolerance. Additionally, hormone-related genes, transcription factors, and protein kinases showed differential expression, suggesting their roles in the differential salt stress response. Enrichment of pathways related to flavonoid biosynthesis and secondary metabolite biosynthesis in PL6 may contribute to its enhanced antioxidant activities. Furthermore, differentially expressed genes associated with the circadian clock system, cytoskeleton organization, and cell wall organization shed light on the plant's response to salt stress.

Conclusion. Understanding these mechanisms is crucial for developing stress-tolerant crop varieties, improving agricultural practices, and breeding salt-resistant crops to enhance global food production and address food security challenges.

1 **Identification and Transcriptomic Profiling of Salinity Stress**
2 **Response Genes in Colored Wheat Mutant**

3

4 Min Jeong Hong¹, Chan Seop Ko¹, Jin-Baek Kim¹

5 ¹ Advanced Radiation Technology Institute, Korea Atomic Energy Research Institute, 29

6 Geungu, Jeongeup 56212, Korea

7

8 Corresponding Author:

9 Dae Yeon Kim²

10 ² Department of Plant Resources, Kongju National University, 54 Daehak-ro Yesan-eup

11 Chungnam 322439, Korea

12 Email Address dykim@kongju.ac.kr

13

14 **Abstract**

15 **Background.** Salinity is a major abiotic stress that prevents normal plant growth and development,
16 ultimately reducing crop productivity. This study investigated the effects of salinity stress on two
17 wheat lines: PL1 (wild type) and PL6 (mutant line generated through gamma irradiation of PL1).

18 **Results.** The salinity treatment was carried out with a solution consisting of a total volume of 200
19 mL containing 150 mM NaCl. Salinity stress negatively impacted germination and plant growth
20 in both lines, but PL6 exhibited higher tolerance. PL6 showed lower Na⁺ accumulation and higher
21 K⁺ levels, indicating better ion homeostasis. Genome-wide transcriptomic analysis revealed
22 distinct gene expression patterns between PL1 and PL6 under salt stress, resulting in notable
23 phenotypic differences. Gene ontology analysis revealed positive correlations between salt stress
24 and defense response, glutathione metabolism, peroxidase activity, and reactive oxygen species
25 metabolic processes, highlighting the importance of antioxidant activities in salt tolerance.
26 Additionally, hormone-related genes, transcription factors, and protein kinases showed differential
27 expression, suggesting their roles in the differential salt stress response. Enrichment of pathways
28 related to flavonoid biosynthesis and secondary metabolite biosynthesis in PL6 may contribute to
29 its enhanced antioxidant activities. Furthermore, differentially expressed genes associated with the
30 circadian clock system, cytoskeleton organization, and cell wall organization shed light on the
31 plant's response to salt stress.

32 **Conclusions.** Understanding these mechanisms is crucial for developing stress-tolerant crop
33 varieties, improving agricultural practices, and breeding salt-resistant crops to enhance global food
34 production and address food security challenges.

35

36 **Introduction**

37 Wheat is a crucial crop cultivated globally, contributing to 30% of global grain production and
38 providing approximately 20% of the calories consumed by humans (*Shiferaw et al., 2013*;
39 *Seleiman et al., 2022*). Soil salinity poses a critical issue, resulting in yield losses of up to 60% in
40 wheat production (*El-Hendawy et al., 2017*). The impact of salinity is extensive, with >20% of
41 irrigated land worldwide being affected (*EL Sabagh et al., 2021*). Furthermore, it is projected that
42 up to 50% of arable land will be lost by 2050 owing to salinization caused by both human activities
43 and ongoing climate change (*Asif et al., 2018*; *Kumar & Sharma, 2020*; *Chele et al., 2021*).

44 Salinity stress disrupts plant growth by increasing Na⁺ ion assimilation and reducing the Na⁺/K⁺
45 ratio, leading to osmotic stress and ion toxicity, consequently affecting normal plant development
46 (*EL Sabagh et al., 2021*). Additionally, under salinity stress, oxidative stress can impair plant
47 growth through reduced photosynthetic capacity, oxidative damage caused by an imbalance in
48 reactive oxygen species (ROS) production, and decreased antioxidant activity, ultimately leading
49 to reduced crop yield (*Hasanuzzaman et al., 2014*; *Sadak, 2019*; *Omrani et al., 2022*).

50 Numerous studies have focused on breeding new salt-tolerant crop varieties using molecular and
51 biotechnologies and on selecting salt-tolerant crops (*Huang et al., 2008*; *Ismail & Horie, 2017*;
52 *Saade et al., 2020*; *Hussain et al., 2021*). These selection criteria encompass germination rate,

53 plant growth, chlorophyll content, and K^+/Na^+ ratio (El-Hendawy et al., 2019; Choudhary et al.,
54 2021; Tsai et al., 2019; Assaha et al., 2017; Singh & Sarkar, 2014). Particularly, the germination
55 and growth rates during the early stages of plant development have proven useful for screening
56 salt-tolerant crops (Choudhary et al., 2021). In *Brassica napus*, root and shoot lengths act as early
57 indicators for evaluating salt tolerance (Long et al., 2015). In rice, salt-tolerant cultivars have
58 higher chlorophyll content and Na^+/K^+ ratios under salt stress conditions than salt-susceptible
59 cultivars (Singh & Sarkar, 2014). Regulating excessive Na^+ accumulation in plants is a vital
60 strategy for enhancing salt resistance (Tester & Davenport, 2003; Møller & Tester, 2007; Møller
61 et al., 2009). The high-affinity K^+ transporter (HKT) gene family plays a crucial role in
62 maintaining Na^+ and K^+ balance in plant growth, development, abiotic stress responses, and salt
63 tolerance (Horie et al., 2009; Li et al., 2019; Riedelsberger et al., 2021). Initially identified in
64 wheat (Schachtman & Schroeder, 1994), HKT genes have been found to reduce Na^+ accumulation
65 in higher plants, such as *Arabidopsis*, rice, and wheat (Riedelsberger et al., 2021). Additionally,
66 the salt overly sensitive (SOS) gene family is involved in regulating ion homeostasis and Na^+
67 exclusion at the cellular level, affecting plant salinity tolerance (Yang et al., 2009).

68 Despite ongoing research on gene regulation under salt stress, limited progress has been made in
69 establishing appropriate screening methods using genetic resources, understanding mechanisms
70 underlying osmotic stress/tissue resistance, and identifying salt-tolerant crops (Genc et al., 2019).
71 Furthermore, as elite germplasm may lack genes that confer salt resistance, genetic engineering
72 involving the artificial insertion of specific genes may be required to develop new crop varieties
73 (Colmer et al., 2006; Shavrukov et al., 2009; Munns et al., 2012; Deinlein et al., 2014).

74 Genetic diversity is crucial for developing new and improved crop varieties with desirable traits.
75 However, breeders often focus on improving traits by selecting offspring with the best attributes,
76 leading to a decrease in genetic diversity when some plants become vulnerable to environmental
77 stresses. Mutation breeding is a widely used method for enhancing genetic diversity and improving
78 crop traits. Gamma rays, being physical mutagens, are commonly used for plant mutation breeding
79 and have been instrumental in developing >50% of the 3,401 new varieties included in the
80 FAO/IAEA Mutant Variety Database (<https://nucleus.iaea.org/sites/mvd/SitePages/Home.aspx>).
81 In light of these findings, the construction of a mutant pool using gamma rays offers an opportunity
82 to develop salt-resistant wheat by securing genetic diversity. This study aims to investigate the
83 changes in the salt tolerance mechanism in the wheat line we developed through gamma-ray
84 mutation. Consequently, the salt-tolerant colored wheat mutant PL6 was selected, and its salt
85 resistance mechanism was scrutinized through transcriptome analysis, comparing PL6 with wild-
86 type wheat (PL1). Colored wheat possesses advantages such as enhanced nutritional content,
87 increased antioxidant levels, and potential health benefits due to its rich phytochemical profile
88 Colored wheat possesses advantages such as enhanced nutritional content, increased antioxidant
89 levels, and potential health benefits due to its rich phytochemical profile (Hong et al., 2019; Garg
90 et al., 2022). The investigation of salt tolerance in colored wheat, characterized by these valuable
91 traits, presents an opportunity to unveil distinctive features that contribute to its resistance against

92 salinity. The findings of this study provide valuable insights into salt tolerance breeding in wheat,
93 offering diverse interpretations of salinity. This comprehensive investigation not only enhances
94 our understanding of the associated molecular mechanisms but also carries practical implications
95 for the development of crops under saline conditions. The findings of this study provide valuable
96 insights for breeding salt-tolerant wheat and offer various interpretations of salt tolerance.

97

98 **Materials & methods**

99 **Plant materials**

100 One of the progenies resulting from the cross between 'Woori-mil' (obtained from the National
101 Agrobiodiversity Center, RDA, Korea; accession no. IT172221) and 'D-7' (an inbred line
102 developed by Korea University; Fleming4/3/PIO2580//T831032/Hamlet) exhibited color
103 segregation. This specific progeny, carefully chosen, had spikes containing colored seeds, and
104 these were utilized in the subsequent generation. Finally, we developed the common wheat
105 (*Triticum aestivum* L., $2n=6x=42$, AABBDD) inbred line K4191 (hereafter termed PL1),
106 distinguished by its deep purple grain color. K4191 was derived from the F4:8 generation resulting
107 from the cross between 'Woori-mil' and 'D-7,' both of which have common seed color (*Hong et*
108 *al.*, 2019). To induce genetic variation and diversity the population of colored wheat, colored
109 wheat seeds (PL1) were irradiated with 200 Gy gamma rays at a dose rate of 25 Gy/h using a ^{60}Co
110 gamma irradiator (150 TBq of capacity; Noridon, Ottawa, ON, Canada) at the Korea Atomic
111 Energy Research Institute. Subsequently, the irradiated seeds were planted at the radiation
112 breeding research farm. Briefly, 1500 M_0 seeds were exposed to irradiation, and the resulting seeds
113 were sown to generate the M_1 generation. Among these seeds, 287 phenotypically distinctive lines
114 were carefully selected with one spike per plant, and mutation breeding spanning from M_0 to M_4
115 was performed as thoroughly described in a previous study (*Hong et al.*, 2019). The resulting
116 mutants were continuously cultivated up to the M_6 generation and carefully selected based on
117 excellent agricultural traits, including flowering time, plant height, yield, and grain color. In total,
118 50 mutant lines displaying stable phenotypes for at least two generations were chosen for further
119 salt-tolerance screening.

120 **Salt stress treatment**

121 The PL1 (control line, K4191) and PL6 (mutant line) seeds were surface-sterilized with 70%
122 ethanol for 1 min and then washed with sterile distilled water. Subsequently, the seeds were placed
123 on moist filter papers in a Petri dish (SPL Life Sciences) until the first leaf of the seedlings
124 appeared. Next, the uniformly germinated seeds were transferred to Incu Tissue culture vessels
125 (SPL Life Sciences) filled with half-strength Hoagland's culture solution (Sigma-Aldrich, St.
126 Louis, MO, USA). The solutions were replaced daily. The seedlings were grown for 7 days in a
127 well-controlled chamber at 22°C and 60% humidity, with a photoperiod regime of 16/8 h day/night
128 at 200–300 $\mu\text{mol m}^{-2}\text{s}^{-1}$ light. After 7 days of transplanting, the seedlings were subjected to a salt
129 stress treatment of a total volume of 200 mL of the solution containing 150 mM NaCl. Following
130 treatment with 150 mM NaCl, the wheat leaves were collected at 0, 3, 24, and 48 h. Both control
131 and salt-stressed seedlings were collected individually. The samples were immediately frozen in
132 liquid nitrogen and stored at -80°C until use in further experiments.

133 Measurement of leaf Na⁺ and K⁺ contents

134 The wheat leaves were collected separately and immediately frozen in liquid nitrogen.
135 Subsequently, the samples were freeze-dried for 3 days in a Freeze Dry System (IlshinBioBase,
136 Dongducheonsi, Gyeonggi, Korea). The freeze-dried samples were then finely ground into a powder
137 using a mortar and pestle. For further analysis, 50 mg of the freeze-dried samples was weighed
138 using an analytical balance and boiled for 2 h at 200°C in 3 mL of HNO₃ (70%, v/v) for digestion.
139 After digestion, the extracted samples were diluted with 5% HNO₃ and filtered through a
140 hydrophilic polytetrafluoroethylene syringe filter (0.45-μM pore size, 25-mm diameter). The shoot
141 Na⁺ and K⁺ contents were measured using inductively coupled plasma atomic emission
142 spectroscopy (ICP-AES, 720 series; Agilent, Santa Clara, CA, USA) and quantitatively analyzed
143 using a VistaChip II CCD detector (Agilent).

144 Measurement of chlorophyll content

145 To determine the chlorophyll content, wheat seedling samples were extracted with 100% methanol
146 at 4°C. The sample extracts were then subjected to centrifugation at 12,000 ×g for 10 min, and the
147 supernatant was used for chlorophyll content analysis. The total chlorophyll, chlorophyll a, and
148 chlorophyll b concentrations were determined by measuring the absorbance at 644.8 and 661.6 nm
149 using a UV-VIS spectrophotometer (*Lichtenthaler, 1987*). The chlorophyll concentration was
150 calculated using the following equations:

$$151 \quad C_a = 11.24 \times A_{661.6} - 2.04 \times A_{644.8}$$

$$152 \quad C_b = 20.13 \times A_{644.8} - 4.19 \times A_{661.6}$$

$$153 \quad C_{\text{total}} = 7.05 \times A_{661.6} + 18.09 \times A_{644.8}$$

154 where C_a, C_b, and C_{total} denote the concentrations of chlorophyll a, chlorophyll b, and total
155 chlorophyll, respectively.

156 RNA sequencing and gene expression analyses

157 Total RNA was extracted from the wheat leaves of both PL1 and PL6 at each timepoint (0, 3, 24,
158 and 48 h) using TRIzol (Invitrogen, Carlsbad, CA, USA) following the manufacturer's
159 instructions. Two independent biological replicates were performed for each timepoint and line to
160 ensure the reliability and reproducibility of the RNA-seq data. Additionally, the extracted RNA
161 samples were treated with DNase I to remove any potential genomic DNA contamination. The
162 RNA quality was assessed using an Agilent 2100 bioanalyzer (Agilent Technologies, Amstelveen,
163 The Netherlands), and RNA quantification was performed using an ND-2000 Spectrophotometer
164 (Thermo Inc.; Wilmington, DE, USA). For constructing the RNA-seq paired-end libraries, 10 μg
165 of total RNA extracted from the samples was used with the TruSeq RNA Sample Preparation Kit
166 (Catalog #RS-122-2001; Illumina, San Diego, CA, USA). The mRNA was isolated using a
167 Poly(A) RNA Selection Kit (LEXOGEN, Inc.; Vienna, Austria) and reverse-transcribed into
168 cDNA following the manufacturer's instructions. The libraries were assessed using the Agilent
169 2100 bioanalyzer, and the mean fragment size was evaluated using a DNA High Sensitivity Kit
170 (Agilent, Santa Clara, CA, USA). High-throughput sequencing was conducted using the HiSeq
171 2000 platform (Illumina). Before alignment, adaptor sequences were removed, and sequence

172 quality was evaluated using the Bbduk tool (minimum length > 20 and Q > 20;
173 <https://jgi.doe.gov/data-and-tools/software-tools/bbtools/bb-tools-user-guide/bbduk-guide/>). The
174 reads were aligned to the wheat genome sequence provided by the International Wheat Genome
175 Sequencing Consortium (IWGSC) wheat reference sequence (IWGSC Reference Sequence v1.0;
176 https://urgi.versailles.inra.fr/download/iwgsc/IWGSC_RefSeq_Annotations/v1.0/) using the
177 HISAT2 alignment program with default parameters (Kim *et al.*, 2015). Reads mapped to the exons
178 of each gene were enumerated using the HTSeq v0.6.1 high-throughput sequencing framework
179 (Anders *et al.*, 2015). Subsequently, the differentially expressed genes (DEGs) under salt stress
180 and control conditions were identified using the EdgeR package (Robinson *et al.*, 2010).
181 Upregulated and downregulated genes with a p-value of <0.05, false discovery rate (FDR) of
182 <0.05, and an absolute fold change value of >2 were used for downstream functional analysis. The
183 log₂-transformed transcript per million values were calculated using TPMCalculator (Vera
184 Alvarez *et al.*, 2019), and heatmaps of DEGs under control and stress conditions were generated.
185 Local BlastX was used with peptide sequences of the Poaceae family retrieved from the National
186 Center for Biotechnology Information (NCBI) database using an e-value threshold of 1×10^{-5} to
187 annotate the DEGs. For gene expression analysis, total RNA was used to synthesize first-strand
188 cDNA using the Power cDNA Synthesis Kit (iNtRON Biotechnology, Gyeonggi-do, Korea).
189 Reverse transcription-quantitative polymerase chain reaction (RT-qPCR) was performed in a total
190 volume of 20 μ L containing 1 μ L of cDNA template, 0.2 μ M primers, and 10 μ L of TB Green
191 Premix Ex Taq II (Takara, Kusatsu, Shiga, Japan). RT-qPCR was conducted using a CFX96TM
192 Real-time PCR system (Bio-Rad, Hercules, CA, USA) with the following program: 95°C for 5
193 min, followed by 40 cycles at 95°C for 10 s and 65°C for 30 s. Actin (AB181991) was used as an
194 internal control. The primers used in this experiment are listed in Table S1.

195 **Functional analysis of DEGs**

196 All expressed genes under both control and stress conditions were subjected to Gene Set
197 Enrichment Analysis (GSEA) using the GSEA software (Subramanian *et al.*, 2005). The gene
198 matrix transposed file format (.GMT) of wheat was downloaded from g:Profiler
199 (<https://biit.cs.ut.ee/gprofiler/gost>), a web server for functional enrichment analysis and gene list
200 conversion (Raudvere *et al.*, 2019). The enrichment score of each gene set was calculated using
201 the full ranking, and the normalized enrichment score (NES) was determined for each gene set.
202 The GSEA results, including rank, expression, and class files, were visualized as a network using
203 Enrichment Map (Merico *et al.*, 2010). For Kyoto Encyclopedia of Genes and Genome (KEGG)
204 pathway enrichment analysis, the KEGG Orthology Database in KOBAS-i was used to predict the
205 putative pathways of DEGs (Bu *et al.*, 2021). The plant transcription factor data were obtained
206 from the Plant Transcription Factor Database (PlantTFDB) (Tian *et al.*, 2020). Protein Basic Local
207 Alignment Search Tool (BLASTP) was used on the peptide sequences of the DEGs, based on the
208 local transcription factor database obtained from PlantTFDB, with an E-value threshold of 1×10^{-1}
209 and sequence identity of >80%. Mev software ([http://sourceforge.net/projects/mev-tm4/files/mev-](http://sourceforge.net/projects/mev-tm4/files/mev-tm4/)
210 [tm4/](http://sourceforge.net/projects/mev-tm4/files/mev-tm4/)) was used for k-means clustering of DEGs identified from the GSEA, KEGG pathway, and
211 transcription factor analyses. The results of the GSEA and KEGG pathway analysis were generated
212 using an R script and the ggplot2 R package. Additionally, MapMan was used to identify the
213 pathways of stage-specific genes (Sreenivasulu *et al.*, 2008).

214 Enzyme activities assays

215 The crude enzyme was extracted from 100 mg of wheat leaves using a protein extraction buffer
216 containing 50 mM potassium phosphate buffer (pH 7.5). The activities of catalase (CAT),
217 peroxidase (POD), and superoxide dismutase (SOD) and total antioxidant activity (TAC) were
218 measured using commercially available assay kits. Specifically, CAT activity was determined
219 using a catalase microplate assay kit (kit number: MBS8243260; MyBiosource, Inc., San Diego,
220 CA, USA), POD activity was measured using a POD assay kit (kit number: KTB1150; Abbkine,
221 Inc., Wuhan, China), and SOD activity was estimated using a total SOD activity assay kit (WST-
222 1 method) (kit number: MBS2540402; MyBiosource, Inc., San Diego, CA, USA). TAC was
223 assessed using a TAC assay kit (kit number: MAK187; Sigma-Aldrich, St. Louis, MO, USA). The
224 preparation of the reaction mixture and the calculations for each measurement were performed as
225 described in the respective protocol books provided with each assay kit.

226

227 Results

228 Characteristics of the salt-tolerant colored wheat mutant induced via gamma irradiation

229 Throughout the mutation breeding process, detailed records of agricultural traits, including the
230 flowering time, plant height, and yield, were meticulously collected for the mutant lines. These
231 data allowed for a comprehensive assessment of the phenotypic characteristics of the lines.
232 Evidence supporting the stable phenotype of the mutant lines is provided in Fig. S1, which also
233 presents the field performance of PL1 and PL6. Additionally, the difference in grain color between
234 the colored wheat lines used in this study is illustrated in Fig. S2. To select salt-resistant wheat
235 lines, 50 wheat mutant lines were treated with 150 mM NaCl, and germination rate, shoot length,
236 and root length were subsequently investigated. The results showed that 27 lines exhibited a
237 germination rate of 90%. Among these, six lines demonstrated a growth increase of approximately
238 20% or more compared to the control group subjected to salt treatment (Fig. S3). Through
239 preliminary salt-tolerance screening, PL6 was selected as the gamma ray-derived mutant line that
240 exhibited favorable salt-tolerance characteristics (Fig.S3). To assess the growth response of the
241 control line (PL1) and PL6 under varying salt concentrations, the seeds were treated with NaCl
242 solutions of 50, 100, 150, 200, 250, 300, and 500 mM, along with distilled water as the control
243 (*Choudhary et al., 2021*). Overall, high salt concentrations negatively affected seed germination
244 and seedling growth (Figs. 1A and 1B). The germination percentage and seedling growth were
245 reduced with increasing salt concentration in both PL1 and PL6 (Table S2). However, PL6
246 demonstrated higher germination percentages, particularly at the maximum NaCl concentration,
247 exceeding those of PL1. Remarkably, a maximum increase of 20% in germination was observed
248 for PL6 following treatment with 250 mM NaCl. Moreover, PL6 consistently outperformed PL1
249 in terms of seedling growth under all salt treatment conditions, as evidenced by its longer shoot
250 and root lengths (Figs. 1C and 1D). The comprehensive data strongly indicates that the gamma
251 ray-derived mutant PL6 exhibits higher resistance to salt stress than PL1.

252 **Assessment of Na⁺, K⁺, and chlorophyll contents under salt stress conditions**

253 Prior to treatment, PL6 had a higher Na⁺ ion content than PL1 (Fig. 2A). However, with increasing
254 time of exposure to salt stress, the Na⁺ ion content markedly increased in both PL1 and PL6.
255 Notably, the rate of increase in Na⁺ ion content was lower in PL6 than in PL1. Conversely, the K⁺
256 ion content steadily decreased with salt treatment in both PL1 and PL6 (Fig. 2B). To further
257 analyze the ion contents, we calculated the relative ratios of K⁺ and Na⁺ ions in PL1 and PL6,
258 considering their respective contents under control conditions (Figs. 2C and 2D). In PL1, the Na⁺
259 ion content increased significantly by 47 times from the baseline (0 h) to 48 h following salt
260 treatment. In contrast, PL6 exhibited a milder increase in Na⁺ ion content, approximately 20 times
261 higher at 48 h after salt stress. Consequently, the relative Na⁺ content was more profoundly
262 affected by salt stress in PL1 than in PL6. Interestingly, the chlorophyll concentrations of both
263 PL1 and PL6 remained relatively stable under salt stress (Fig. 2E), indicating that they were not
264 significantly affected by the imposed salinity conditions.

265 **DEGs during salt stress**

266 After treatment with 150 mM NaCl, leaves were harvested from PL1 and PL6 at 0, 3, 24, and 48
267 h and subjected to RNA sequencing. Following quality evaluation and trimming, an average of
268 38.1 million trimmed reads and over 22.1 billion bases were generated from each sample under
269 both control and salt stress conditions. The average percentage of Q20 and Q30 bases was found
270 to be 98.4% and 95.5%, respectively, indicating high sequencing quality. Moreover, >96% of the
271 sequenced data exhibited an average mapping rate of 96.16%, successfully aligning to the IWGSC
272 wheat reference sequence (Table S3). During data analysis, a total of 4,017 DEGs were identified
273 with a p-value of <0.05, FDR of <0.05, and absolute fold change value of >2 (Fig. 3A and Table
274 S4). Specifically, in PL1, 872, 1,588, and 1,080 DEGs were identified at 3, 24, and 48 hours after
275 salt treatment, respectively, in comparison to the untreated condition (0h) (Fig. 3B). Similarly, for
276 PL6, the number of DEGs was 566, 1,248, and 1,810 at 3, 24, and 48 hours after salt treatment,
277 respectively (Fig. 3C). These results highlight the dynamic gene expression changes in PL1 and
278 PL6 under salt stress at different timepoints, contributing to a better understanding of the
279 underlying molecular responses to salt stress in these wheat lines.

280 **Functional analysis of the DEGs during salt stress**

281 Overall, 33 GO terms were identified for each treatment condition (Fig. 3D and Table S5).
282 Notably, several gene sets, including defense response (GO: 0006952), glutathione metabolic
283 process (GO: 0006749), peroxidase activity (GO: 0004601), ROS metabolic process (GO:
284 0072593), response to biotic stimulus (GO: 0009607), and response to stress (GO: 0006950), were
285 positively correlated with salt stress and PL6, exhibiting a positive NES (Fig. 3D). To visualize
286 the results, all the gene sets from the GSEA were organized into four networks using Enrichment
287 Map (*Merico et al., 2010*) (Figs. 4A–4E). The expression patterns of each network in Figs. 4A–
288 4E for PL1 and PL6 were clustered by expressed patterns (Figs. 4F–4J, respectively). The K-means
289 clustering algorithm in the Mev software was used to identify the clusters of DEGs in each GO
290 term under control and salt stress conditions based on their expression patterns. Most of the
291 expression patterns from the identified clusters did not differ between the control and salt stress
292 conditions. Three clusters that demonstrated different expression patterns for PL1 and PL6,
293 especially those upregulated in PL6, were selected and marked in red boxes in Figs. 4F, 4G, and

294 4I, and a heatmap of the genes from these clusters was generated (Fig. 4K). Plant hormone-related
295 genes (*TRAESCS1B02G145800* and *TRAESCS1B02G138100*), ROS-related genes
296 (*TRAESCS1B02G059100*, *TRAESCS1B02G095800*, *TRAESCS1B02G096200*,
297 *TRAESCS1B02G096900*, and *TRAESCS1B02G115900*), and stress-response genes
298 (*TRAESCS5D02G492900*, *TRAESCS1A02G009900*, *TRAESCS1B02G023000*, and
299 *TRAESCS2A02G037400*) were highly expressed in PL6 under salt stress conditions. Furthermore,
300 six genes related to chromatin remodeling (*TRAESCS1B02G048900*, *TRAESCS1B02G049100*,
301 *TRAESCS1D02G286700*, *TRAESCS1B02G149000*, and *TRAESCS7D02G246600*) showed high
302 expression patterns in PL6 under salt stress conditions [Table 1]. A high number of transcriptomes
303 of MADS-box transcription factors (*TRAESCS4A02G002600*, and *TRAESCS6D02G293200*) were
304 also detected in PL6 under salt stress. An auxin-responsive protein (*TRAESCS1B02G138100*) and
305 probable histone H2A variant 3 (*TRAESCS7D02G246600*) were also found in cluster 4 [Table 1].

306 In the case of the differences in the KEGG pathways between PL1 and PL6 under salt stress
307 conditions, the rich factor of “Biosynthesis of secondary metabolites” in PL6 after 3 h of salt stress
308 was ~ 0.05 , increasing to ~ 0.2 after 48 h of salt stress (Fig. 5). Likewise, the rich factors of
309 “Flavonoid biosynthesis” were 0.17 and 0.23, after 24 and 48 h of salt stress, respectively. This
310 was only observed in PL6 during salt stress conditions (Fig. 5 and Table S6).

311 In addition to GO and KEGG analysis, the role of DEGs as transcription factors was investigated.
312 DEGs at different timepoints under salt stress in PL1 and PL6 were identified using PlantTFDB
313 (<http://planttfdb.gao-lab.org>). In total, 255 genes were identified with an e-value threshold of $1 \times$
314 10^{-1} and a sequence identity of $>80\%$ and further selected to compare the expression patterns
315 between PL1 and PL6 under salt stress conditions. The most abundant type of transcription factor
316 was the ethylene-response factor (ERF) protein family, followed by the basic helix-loop-helix
317 (bHLH) protein family; heat shock transcription factor protein family; myeloblastosis (MYB)-
318 related protein family; and Nam, ATAF, and CUC (NAC) protein family (Fig. 6A). Moreover, 255
319 putative transcription factors were grouped by expression pattern into six clusters and an
320 unclassified group (Fig. 6B). Overall, 72, 44, and 35 DEGs were annotated by the ERF, bHLH,
321 and MYB (related) protein families, respectively. These three transcription factors accounted for
322 59% of the total number of transcription factors. The expression patterns of DEGs in clusters 2
323 and 6 (marked with red boxes in Fig. 6B) were selected and expressed in heatmaps (Fig. 6C) to
324 display differences in the expression patterns of DEGs between PL1 and PL6 under salt stress
325 conditions (Table S7). Notably, PL6 exhibited higher expression of specific transcription factors
326 under salt stress conditions than PL1, as displayed in the heatmap (Fig. 6C).

327 Lastly, 22 protein kinase genes were identified with significant expression patterns at different
328 timepoints, including two calcineurin B-like (CBL)-interacting protein kinases and one mitogen-
329 activated protein kinase (MAPK) with more than two-fold changes in PL6 under salt stress (Table
330 2). Additionally, 70 differentially expressed salt stress-responsive genes involved in regulating the
331 circadian clock system, cytoskeleton organization, and cell wall organization were identified using
332 MapMan, with 15 of them showing more than a two-fold change in PL6 (Table 3).

333 Enzyme activities assays

334 To investigate the differences in enzyme activities between PL1 and PL6 under salt stress
335 conditions, we measured CAT, POD, and SOD activities and TAC (Fig. 7). Upon subjecting both
336 wheat lines to salt stress, we observed distinct patterns in enzyme activities. In PL6, CAT and POD

337 activities significantly increased after 24 and 48 h of exposure to salt stress (Fig. 7A and B).
338 Conversely, in PL1, SOD activity slightly decreased after 24 and 48 h exposure to salt stress (Fig.
339 7C). Furthermore, the TAC in PL1 was not significantly changed by salt stress (Fig. 7D).
340 Conversely, in PL6, the TAC notably increased after 24 and 48 h of exposure to salt stress. This
341 increase in TAC suggests that PL6 has a higher capacity to counteract oxidative stress and maintain
342 cellular redox balance than PL1, contributing to its enhanced salinity tolerance.

343 **Validation of the DEG results using reverse transcription-quantitative polymerase chain** 344 **reaction**

345 Supporting the DEG results, 12 genes from the three aforementioned clusters from PL1 and PL6
346 were selected for RT-qPCR (Fig. 8). All the selected genes were more highly expressed in PL6
347 than in PL1. *peroxidase 2* (TRAESCS1B02G095800), *nitrate transporter*
348 (TRAESCS1B02G038700), *auxin-responsive protein* (TRAESCS1B02G138100), and *replication*
349 *protein A* (TRAESCS1B02G102200) transcripts in PL6 were highly expressed at 48 h following
350 salt treatment (Fig. 8A). *Nuclear transport factor 2- like protein* (TRAESCS2A02G046200),
351 *histone H2A* (TRAESCS1B02G048900), *integral membrane protein* (TRAESCS1B02G071800),
352 and *histone H2A variant 3* (TRAESCS7D02G246600) transcripts in PL6 continuously decreased
353 at 24 h and peaked at 48 h following salt treatment (Fig. 8B). *Argonaute 1C-like isoform X2*
354 (TRAESCS6B02G466700), *MADS-box* (TRAESCS6B02G017900), and *aspartokinase 1*
355 (TRAESCS5D02G537600) transcripts in PL6 peaked at 3 h, and all gradually decreased, except
356 for *ribosome biogenesis protein NOP53* (TRAESCS1B02G105100) (Fig. 8C). These results are
357 consistent with those of RNA sequencing (RNA-seq).

358

359

360 **Discussion**

361 This study revealed that salinity stress had negative effects on germination and plant growth during
362 the developmental process. Na⁺ is considered a nonessential element in plants (Nieves-Cordones
363 *et al.*, 2016); however, excessive accumulation of Na⁺ can have detrimental effects on plants,
364 including disrupting cellular homeostasis, inducing oxidative stress, and suppressing growth
365 (Munns & Tester, 2008; Craig Plett, 2010). In this study, PL6 consistently showed higher
366 germination rates and better seedling growth under salt stress than PL1. The differences in K⁺ and
367 Na⁺ contents between PL1 and PL6 supported these observations, highlighting PL6's superior
368 performance under salt treatment conditions. Previous studies have emphasized the significance
369 of maintaining a low sodium concentration and a high K⁺/Na⁺ ratio as crucial traits in plant salt
370 tolerance (Ismail & Horie, 2017; Naeem *et al.*, 2020). Salinity triggers osmotic stress, resulting in
371 accumulation of higher salt levels in cell sap and tissues (EL Sabagh *et al.*, 2021). This
372 accumulation is directly linked to the buildup of Na⁺ and Cl⁻, causing ion imbalance that adversely
373 affects germination and subsequent metabolic processes (Hussain *et al.*, 2019). Genome-wide
374 transcriptomic analysis has emerged as a powerful tool to investigate stress-tolerant genes, gene
375 families, and related mechanisms in plants (Peng *et al.*, 2014; Li *et al.*, 2016). In this study, we
376 observed a significant difference in the salinity response between PL1 and PL6 and identified
377 distinct expression patterns of DEGs between the two lines. Although a higher number of DEGs

378 was found in PL6 compared with PL1, it is important to note that the majority of these DEGs
379 exhibited similar expression patterns in both PL1 and PL6 under salt stress conditions. This could
380 be because PL6 was generated through a mutation of PL1 via gamma irradiation, leading to the
381 sharing of numerous genomes between them. Nonetheless, despite the similar expression patterns,
382 clear phenotypic differences were observed, including variations in germination rate, shoot and
383 root growth, and ion concentrations (Na^+ and K^+). Thus, our genome-wide transcriptional analysis
384 allowed us to identify the DEGs responsible for the differential responses of PL1 and PL6 under
385 salt stress conditions.

386 Salt stress not only induces osmotic stress but also leads to ionic imbalance, resulting in ion toxicity
387 and, ultimately, the production of ROS (Julkowska & Testerink, 2015). In our study, PL1 (as the
388 wild-type line) exhibited a dark-purple seed coat and had high levels of anthocyanin, phenolic
389 compounds, and antioxidant activities (Hong *et al.*, 2019). Similarly, PL6, which was generated
390 by irradiating PL1 with 200 Gy of gamma rays, also displayed a dark-purple seed coat.

391 As shown in Figure 3D, GSEA revealed several GO terms that were positively correlated with salt
392 stress, including defense response (GO: 0006952), glutathione metabolic process (GO: 0006749),
393 peroxidase activity (GO: 0004601), ROS metabolic process (GO: 0072593), response to biotic
394 stimulus (GO: 0009607), and response to stress (GO:0006950). Among these terms, three were
395 specifically related to antioxidant activity: glutathione metabolic process (GO: 0006749),
396 peroxidase activity (GO: 0004601), and ROS metabolic process (GO: 0072593). These
397 antioxidant-related GO terms are crucial protective mechanisms against salinity stress in plants.
398 Interestingly, we observed that DEGs related to antioxidants were specifically upregulated in PL6
399 48 h after salt stress, despite both PL1 and PL6 having colored seed coats. This suggests that these
400 DEGs may positively contribute to salt stress tolerance, leading to more vigorous shoot and root
401 growth in PL6 than that in PL1. In addition to the gene expression analysis, the measurement of
402 antioxidant enzyme activities further supports the higher antioxidant capacity in PL6 than in PL1
403 under salt stress conditions. CAT and POD activities were significantly increased at 24 and 48 h
404 after salt stress exposure in PL6 (Fig. 7A and B), indicating efficient ROS-scavenging ability and
405 peroxide detoxification, which help protect the cells from oxidative damage during salt stress.
406 Conversely, in PL1, SOD activity slightly decreased at 24 and 48 h post-salt stress (Fig. 7C),
407 suggesting a limited ability to efficiently neutralize superoxide radicals, potentially leading to ROS
408 accumulation and oxidative stress in PL1 under salt stress conditions. Overall, these findings not
409 only provide insights into the DEGs related to antioxidant activity but also highlight the distinctive
410 enzymatic responses to salt stress in PL1 and PL6. The increases in CAT and POD activities and
411 TAC in PL6 might play crucial roles in its superior ability to manage salt-induced oxidative stress
412 compared with the wild-type PL1. The combination of gene expression analysis and antioxidant
413 enzyme activity measurements sheds light on the activation of specific antioxidant pathways in
414 PL6, providing a comprehensive understanding of its enhanced salinity stress response.

415 Phytohormones, such as abscisic acid (ABA) and auxins (indole acetic acid [IAA] and indole-3-
416 butyric acid), play crucial roles in plant responses to environmental stresses, including salinity.

417 ABA promotes ABA-dependent and reactive oxygen species ROS-related stress signaling
418 mechanisms, conferring salinity tolerance in wheat (*Dong et al., 2013*). IAA play an important
419 role in the metabolism of plants by increasing the activity of enzymes responsible for biosynthesis
420 of growth promoters under saline stress in wheat (*Hendawey, 2015*). In this study, we observed
421 increased transcription levels of TRAESCS1B02G145800 (ABA receptor PYL8) and
422 TRAESCS1B02G138100 (auxin-responsive protein IAA15) in PL6 under salt stress conditions
423 (Table 1). Additionally, salinity-induced osmotic stress leads to the overproduction of ROS and
424 oxidative damage to plant cells. To counteract this, the antioxidant defense system in plants is
425 activated to detoxify ROS and maintain redox homeostasis (*Hasanuzzaman et al., 2021*).
426 Accordingly, we found that plant hormone-related genes, including dehydroascorbate reductase
427 and peroxidase genes, were upregulated in PL6 under salt stress to protect against ROS-induced
428 damage and maintain cellular redox balance (Table 1). The increased expression of ROS-related
429 genes in PL6 suggests that this mutant line may exhibit an altered response to salt stress-induced
430 oxidative stress.

431 In addition to hormone-related responses, transcriptional regulation through histone modification
432 and chromatin remodeling plays a pivotal role in plant responses to salt stress. In this study, we
433 observed an increase in the transcription levels of INO80 complex subunit D
434 (TRAESCS1B02G149000) in PL6 under salt stress conditions. The INO80 chromatin remodeling
435 complex is responsible for evicting the histone variant H2A.Z in eukaryotic cells (*Alatwi & Downs,*
436 *2015*). Studies in *Arabidopsis* have demonstrated that under salt stress, the INO80 complex induces
437 the eviction of H2A.Z-containing nucleosomes from the AtMYB44 promoter region, leading to
438 increased accumulation of AtMYB44 transcripts and thus promoting salt stress tolerance (*Nguyen*
439 *& Cheong, 2018*). However, the specific target gene and position of the histone variant H2A.Z
440 evicted by the INO80 complex in wheat remain unclear. Further investigations are required to
441 identify the precise position of H2A.Z evicted by the INO80 complex and clarify the factors
442 influencing the differential responses of PL1 and PL6 to salinity stress.

443 Moreover, investigation of the MADS-box family members contributes to our understanding of
444 the differential responses of PL1 and PL6 to salinity stress. MADS-box transcription factors are
445 known to regulate flowering development (*Lee & Lee, 2010; Callens et al., 2018*). *Wu et al. (2020)*
446 reported that overexpression of *OsMADS25* in rice and *Arabidopsis* resulted in improved salinity
447 tolerance compared with that in the wild-type. Conversely, the MADS-box transcription factor
448 *AGL16* was identified as a negative regulator of stress responses in *Arabidopsis* (*Zhao et al., 2021*).
449 In this study, we observed increased transcription levels of two MADS-box transcription factors
450 (TRAESCS4A02G002600 and TRAESCS6D02G293200) in PL6 mutant plants under salt stress
451 conditions, suggesting their potential roles in salt tolerance and growth response. These findings
452 provide valuable insights into the molecular mechanisms underlying the differential responses of
453 PL1 and PL6 to salinity.

454 Furthermore, although GO terms related to photosynthesis were detected via GSEA and network
455 analysis (Figs. 3D and 4B), no significant differences were observed in the gene expression

456 patterns between PL1 and PL6. This finding is consistent with the data on chlorophyll
457 concentration (Fig. 2E), which did not show significant variation between PL1 and PL6 during the
458 duration of salt stress exposure. In our previous study, we observed that the total anthocyanin
459 concentrations in wheat mutant lines (used in this study) were significantly higher than those in
460 wild-type lines, resulting in higher antioxidant activity in the mutants compared with the wild-type
461 (*Hong et al., 2019*). In the present study, the enriched factors “Biosynthesis of secondary
462 metabolites” and “Flavonoid biosynthesis” increased following salt stress treatment (Fig. 5). This
463 suggests that the antioxidant activities of PL6 under salt stress conditions might be influenced by
464 these pathways, which include genes associated with GO terms such as glutathione metabolic
465 process (GO: 0006749), peroxidase activity (GO: 0004601), and ROS metabolic process (GO:
466 0072593) (Fig. 3D).

467 As shown in Fig. 4D, several DEGs were mapped to GO terms related to gene expression
468 regulation (GO: 001046), DNA binding transcription factor activity (GO: 0003700), and
469 transcription regulator activity (GO: 0140110). To elucidate the molecular mechanism of salt stress
470 response at the cellular level, we analyzed putative transcription factors and selected those with
471 differential expression patterns in PL6 under salt stress conditions. Among them, the ERF family
472 protein emerged as an important family of transcription factors in plants, regulating various
473 developmental processes (*Nakano, 2006*), including their response to salt stress (*Cheng et al.,*
474 *2013; Li et al., 2020b; Trujillo et al., 2008*). Additionally, studies have revealed the significance
475 of the bHLH and MYB gene families in the response to salt stress in plants (*Yang et al., 2021; Li*
476 *et al., 2020a; Jiang et al., 2009; Kim et al., 2013; Seo et al., 2012*). The putative transcription
477 factors shown in Fig. 6 can be further analyzed for their functions to better understand the
478 molecular mechanisms of salt response. Flavonoid biosynthesis has been extensively studied and
479 is predominantly regulated at the transcriptional level by the MYB–bHLH–WD40 complex in
480 various plant species, such as rice, *Arabidopsis*, *Mimulus*, apples, and maize (*Tohge et al., 2017;*
481 *An et al., 2020; Yuan et al., 2014; Zheng et al., 2019; Baudry et al., 2006*). In this study, several
482 bHLH and MYB gene families were identified as putative transcription factors, likely influenced
483 by the seed colors of PL1 (wild-type) and PL6 (mutant line) used in the experiment. Consequently,
484 based on the heat map in Fig. 6, the bHLH and MYB gene families exhibiting different expression
485 patterns between PL1 and PL6 were considered differentially expressed transcription factors under
486 salt stress conditions.

487 Moreover, protein kinases play a vital role in regulating plant responses to salt stress. *Jin et al*
488 *(2016)* investigated the expression levels of protein kinase genes in response to salt stress in
489 transgenic wheat. They found that overexpression of *TaCIPK25* resulted in hypersensitivity to Na^+
490 and superfluous accumulation of Na^+ in transgenic wheat lines. Similarly, the overexpressed
491 *TMPK3* (*Triticum aestivum* Mitogen Activated Protein Kinase) promotes salt and osmotic stress
492 tolerance to levels exceeding those observed in wild type plants. This tolerance is associated to a
493 lower sensitivity to exogenous ABA, and increased stronger accumulation of proline contents,
494 higher survival, and lower water loss rates as well as attenuated oxidative stress status (*Ghorbel et*

495 *al.*, 2023). These findings underscore the importance of protein kinases in the regulation of plant
496 responses to salt stress and suggest that different types of protein kinases play specific roles in
497 these processes.

498 In the present study, we identified 15 DEGs with more than a two-fold change, among which one,
499 five, and nine genes were involved in the circadian clock system, cytoskeleton organization, and
500 cell wall organization, respectively (Table 3). These processes play crucial roles in plant stress
501 response and are important components of how plants adapt to challenging environments. The
502 circadian clock system has been found to be essential in regulating the plant's response to salt
503 stress. *Xu et al.* (2022) conducted a study on *Arabidopsis* plants and demonstrated that the circadian
504 clock system is involved in the modulation of salt stress responses. They observed altered
505 expression levels of circadian clock genes under salt stress conditions and further noted that the
506 disruption of the circadian clock system resulted in reduced salt tolerance in the plants. Likewise,
507 the cytoskeleton organization is also critical for regulating plant responses to salt stress. For
508 instance, in rice plants, the actin cytoskeleton has been shown to play a role in regulating the
509 response to salt stress, ion homeostasis, and ROS scavenging (*Chun et al.*, 2021). Disruption of
510 the actin filaments in rice plants led to reduced salt tolerance, indicating the importance of the
511 cytoskeleton in coping with salt-induced stress. Moreover, the cell wall organization is a vital
512 aspect of the response of maize to salt stress. A study on maize revealed that the expression of
513 genes related to the cell wall was altered under salt stress conditions, and modification of the cell
514 wall composition contributed to increased salt tolerance in the plants (*Oliveira et al.*, 2020). These
515 findings highlight the significance of the cell wall in mediating the plant's ability to withstand salt
516 stress.

517 The primary focus of this study was to investigate the molecular mechanisms underlying salinity
518 stress responses in the colored wheat mutant PL6 through transcriptomic profiling of leaf tissues.
519 However, considering the crucial role of roots in nutrient and mineral absorption, examining the
520 variations in Na⁺ and K⁺ levels in root tissues could provide valuable insights into tissue-specific
521 ion absorption and accumulation mechanisms in PL6. Furthermore, conducting a comprehensive
522 analysis of DEGs in root tissues could reveal novel genes and pathways associated with salt stress
523 responses that significantly contribute to the enhanced tolerance observed in PL6. Further research
524 incorporating histological analyses of root tissues and transcriptomic profiling of roots would be
525 instrumental in unraveling the genetic basis and tissue-level adaptations responsible for the
526 superior salt stress response and tolerance of PL6.

527

528 **Conclusions**

529 In conclusion, this investigation of the effects of salinity stress on two wheat lines, namely PL1
530 (wild-type) and PL6 (mutant line generated through gamma irradiation of PL1), revealed that salt
531 stress negatively affected germination and plant growth in both lines. However, PL6 demonstrated
532 greater tolerance to salinity stress than PL1, indicating that the mutant line has acquired

533 mechanisms to more effectively mitigate salt stress-induced damage. The differences in ion
534 concentrations observed in PL6, including lower Na⁺ levels and higher K⁺ levels, suggest better
535 ion homeostasis in this line, contributing to its enhanced salt stress tolerance. Our genome-wide
536 transcriptomic analysis provided insights into the differential expression patterns of genes between
537 PL1 and PL6 under salt stress conditions, leading to the observed phenotypic differences. Several
538 GO terms related to defense responses, glutathione metabolism, peroxidase activity, and ROS
539 metabolic processes were positively correlated with salt stress, highlighting the importance of
540 antioxidant activities in salt tolerance. The specific upregulation of DEGs related to antioxidants
541 in PL6, despite both lines having colored seed coats, suggests that these DEGs play critical roles
542 in enhancing salt stress tolerance and promoting vigorous shoot and root growth. Additionally,
543 hormone-related genes, transcription factors, and protein kinases displayed differential expression,
544 indicating their involvement in the differential salt stress responses between PL1 and PL6. The
545 enrichment of pathways related to flavonoid biosynthesis and secondary metabolite biosynthesis
546 in PL6 further suggests their contribution to the enhanced antioxidant activities observed in this
547 line. It is important to acknowledge that the mechanisms underlying salt stress resistance in plants
548 are highly complex and not easily discernible. The interplay of various genetic, physiological, and
549 biochemical factors contributes to the overall response to salinity stress, making it challenging to
550 draw straightforward conclusions. Nevertheless, understanding these intricate mechanisms is
551 crucial for developing stress-tolerant crop varieties and improving agricultural practices. By
552 gaining insights into the genes and pathways responsible for salt stress tolerance, researchers can
553 design targeted breeding programs to develop salt-resistant crop varieties, thereby enhancing
554 global food production and addressing food security challenges.

555

556 **References**

557 **An JP, Wang XF, Zhang XW, Xu HF, Bi SQ, You CX, Hao YJ. 2020.** An apple Myb
558 transcription factor regulates cold tolerance and anthocyanin accumulation and undergoes
559 Miell1-mediated degradation. *Plant Biotechnology Journal* **18(2)**:337–353 DOI
560 10.1111/pbi.13201.

561 **Anders S, Pyl PT, Huber W. 2015.** Htseq—A python framework to work with high-throughput
562 sequencing data. *Bioinformatics* **31(2)**: 166–169 DOI 10.1093/bioinformatics/btu638.

563 **Asif MA, Schilling RK, Tilbrook J, Brien C, Dowling K, Rabie H, Short L, Trittermann C,
564 Garcia A, Barrett-Lennard E, Berger B, Mather DE, Gilliam M, Fleury D, Tester M, Roy
565 SJ, Pearson AS. 2018.** Mapping of novel salt tolerance QTL in an Excalibur × Kukri doubled
566 haploid wheat population. *TAG. Theoretical and Applied Genetics* **131**:2179–2196 DOI
567 10.1007/s00122-018-3146-y.

568 **Assaha DVM, Ueda A, Saneoka H, Al-Yahyai R, Yaish MW. 2017.** The role of Na⁺ and K⁺
569 transporters in salt stress adaptation in glycophytes. *Frontiers in Physiology* **8**:509 DOI
570 10.3389/fphys.2017.00509.

571 **Baudry A, Caboche M, Lepiniec L. 2006.** Tt8 controls its own expression in a feedback
572 regulation involving Ttg1 and homologous Myb and bHLH factors, allowing a strong and

- 573 cell-specific accumulation of flavonoids in *Arabidopsis thaliana*. *The Plant Journal* **46(5)**:768–
574 779 DOI 10.1111/j.1365-313X.2006.02733.x.
- 575 **Callens C, Tucker MR, Zhang D, Wilson ZA. 2018.** Dissecting the role of MADS-box genes in
576 monocot floral development and diversity. *Journal of Experimental Botany* **69(10)**: 2435–2459
577 DOI 10.1093/jxb/ery086.
- 578 **Chele KH, Tinte MM, Piater LA, Dubery IA, Tugizimana F. 2021.** Soil salinity, a serious
579 environmental issue and plant responses: A metabolomics perspective. *Metabolites* **11(11)**:724
580 DOI 10.3390/metabo11110724.
- 581 **Cheng MC, Liao PM, Kuo WW, Lin TP. 2013.** The *Arabidopsis* ethylene response Factor1
582 regulates abiotic stress-responsive gene expression by binding to different cis-acting elements in
583 response to different stress signals. *Plant Physiology* **162(3)**:1566–1582 DOI
584 10.1104/pp.113.221911.
- 585 **Choudhary A, Kaur N, Sharma A, Kumar A. 2021.** Evaluation and screening of elite wheat
586 germplasm for salinity stress at the seedling phase. *Physiologia Plantarum* **173(4)**:2207–2215 DOI
587 10.1111/ppl.13571.
- 588 **Chun HJ, Baek D, Jin BJ, Cho HM, Park MS, Lee SH, Lim LH, Cha YJ, Bae DW, Kim ST,
589 Yun DJ, Kim MC. 2021.** Microtubule dynamics plays a vital role in plant adaptation and tolerance
590 to salt stress. *International Journal of Molecular Sciences* **22(11)**:5957 DOI
591 10.3390/ijms22115957.
- 592 **Colmer T D, Flowers, T J, Munns R. 2006.** Use of wild relatives to improve salt tolerance in
593 wheat. *Journal of Experimental Botany* **57(5)**:1059–1078 DOI 10.1093/jxb/erj124.
- 594 **Deinlein U, Stephan AB, Horie T, Luo W, Xu G, Schroeder J I. 2014.** Plant salt-tolerance
595 mechanisms. *Trends in Plant Science* **19(6)**:371–379 DOI 10.1016/j.tplants.2014.02.001.
- 596 **Dong W, Wang M, Xu F, Quan T, Peng K, Xiao L, Xia G. 2013.** Wheat oxophytodienoate
597 reductase gene *TaOPR1* confers salinity tolerance via enhancement of abscisic acid signaling and
598 reactive oxygen species scavenging. *Plant Physiology* **161**:1217–1228 DOI:
599 10.1104/pp.112.211854.
- 600 **El-Hendawy S. E, Hassan WM, Al-Suhaibani NA, Refay Y, Abdella KA. 2017.** Comparative
601 performance of multivariable agro-physiological parameters for detecting salt tolerance of wheat
602 cultivars under simulated saline field growing conditions. *Frontiers in Plant Science* **8**:435 DOI
603 10.3389/fpls.2017.00435.
- 604 **El-Hendawy S, Elshafei A, Al-Suhaibani N, Alotabi M, Hassan W, Dewir YH, Abdella K.
605 2019.** Assessment of the salt tolerance of wheat genotypes during the germination stage based on
606 germination ability parameters and associated SSR markers. *Journal of Plant Interactions*
607 **14(1)**:151–163 DOI 10.1080/17429145.2019.1603406.
- 608 **EL Sabagh A, Islam MS, Skalicky M, Ali Raza M, Singh K, Anwar Hossain M, Mahboob W,
609 Iqbal MA, Ratnasekera D, Singhal RK, Ahmed S, Kumari A, Wasaya A, Sytar O, Brestic M,
610 ÇIG F, Erman M, Habib Ur Rahman M, Ullah N, Arshad A. 2021.** Salinity stress in wheat
611 (*Triticum aestivum* L.) in the changing climate: Adaptation and management strategies. *Frontiers
612 in Agronomy* **3**:661932 DOI 10.3389/fagro.2021.661932.

- 613 **Garg M, Kaur S, Sharma A, Kumari A, Tiwari V, Sharma S, Kapoor P, Sheoran B, Goyal**
614 **A, Krishania M. 2022.** Rising demand for healthy foods-anthocyanin biofortified colored wheat
615 is a new research trend. *Frontiers in Nutrition* **9**:878221 DOI 10.3389/fnut.2022.878221.
- 616 **Genç Y, Taylor J, Lyons G, Li Y, Cheong J, Appelbee M, Oldach K, Sutton T. 2019.** Bread wheat
617 with high salinity and sodicity tolerance. *Frontiers in Plant Science* **10**:1280 DOI
618 10.3389/fpls.2019.01280.
- 619 **Ghorbel M, Zaidi I, Ebel C, Brini F, Hanin M. 2023.** The wheat Mitogen Activated Protein
620 Kinase TMPK3 plays a positive role in salt and osmotic stress response. *Acta Physiologiae*
621 *Plantarum* **45(6)**:71 DOI 10.1007/s11738-023-03548-1.
- 622 **Hasanuzzaman M, Alam MM., Rahman A, Hasanuzzaman M, Nahar K, Fujita M. 2014.**
623 Exogenous proline and glycine betaine mediated upregulation of antioxidant defense and
624 glyoxalase systems provides better protection against salt-induced oxidative stress in two rice
625 (*Oryza sativa* L.) varieties. *BioMed Research International* **2014**: Article ID 757219 DOI
626 10.1155/2014/757219.
- 627 **Hasanuzzaman M, Raihan MRH, Masud AAC, Rahman K, Nowroz F, Rahman M, Nahar**
628 **K, Fujita M. 2021.** Regulation of reactive oxygen species and antioxidant defense in plants under
629 salinity. *International Journal of Molecular Sciences* **22(17)**:9326 DOI 10.3390/ijms22179326.
- 630 **Hendawey, MH. 2015.** Biochemical changes associated with induction of salt tolerance in wheat.
631 *Global Journal of Biotechnology & Biochemistry* **10(2)**: 84-99 DOI
632 10.5829/idosi.gjbb.2015.10.02.1120.
- 633 **Hong MJ, Kim DY, Nam BM, Ahn JW, Kwon SJ, Seo YW, Kim JB. 2019.** Characterization
634 of novel mutants of hexaploid wheat (*Triticum aestivum* L.) with various depths of purple grain
635 color and antioxidant capacity. *Journal of the Science of Food and Agriculture* **99(1)**:55–63 DOI
636 10.1002/jsfa.9141.
- 637 **Horie T, Hause, F, Schroeder JI. 2009.** HKT transporter-mediated salinity resistance
638 mechanisms in *Arabidopsis* and monocot crop plants. *Trends in Plant Science* **14(12)**:660–668
639 DOI 10.1016/j.tplants.2009.08.009.
- 640 **Huang S, Spielmeier W, Lagudah ES, Munns, R. 2008.** Comparative mapping of HKT genes
641 in wheat, barley, and rice, key determinants of Na⁺ transport, and salt tolerance. *Journal of*
642 *Experimental Botany* **59(4)**:927–937. DOI 10.1093/jxb/ern033.
- 643 **Hussain N, Ghaffar A, Zafar ZU, Javed M, Shah KH, Noreen S, Manzoor H, Iqbal M,**
644 **Hassan IFZ, Bano H, Gul HS, Aamir M, Khalid A, Sohail Y, Ashraf M, Athar H. U. R. 2021.**
645 Identification of novel source of salt tolerance in local bread wheat germplasm using morpho-
646 physiological and biochemical attributes. *Scientific Reports* **11**:10854. DOI 10.1038/s41598-021-
647 90280-w.
- 648 **Hussain S, Shaukat M, Ashraf M, Zhu C, Jin Q, Zhang J. 2019.** Salinity stress in arid and
649 semi-arid climates: Effects and management in field crops. *Climate Change and Agriculture.*
650 *IntechOpen* 125-145 DOI 10.5772/intechopen.87982.

- 651 **Ismail AM, Horie T. 2017.** Genomics, physiology, and molecular breeding approaches for
652 improving salt tolerance. *Annual Review of Plant Biology* **68**:405–434. DOI 10.1146/annurev-
653 arplant-042916-040936.
- 654 **Jiang Y, Yang B, Deyholos MK. 2009.** Functional characterization of the *Arabidopsis* bHLH92
655 transcription factor in abiotic stress. *Molecular Genetics and Genomics* **282**:503–516. DOI
656 10.1007/s00438-009-0481-3.
- 657 **Jin X, Sun T, Wang X, Su P, Ma J, He G, Yang G. 2016.** Wheat CBL-interacting protein kinase
658 25 negatively regulates salt tolerance in transgenic wheat. *Scientific reports* **6(1)**:28884 DOI
659 10.1038/srep28884.
- 660 **Julkowska MM, Testerink C. 2015.** Tuning plant signaling and growth to survive salt. *Trends in*
661 *Plant Science* **20(9)**:586–594. DOI 10.1016/j.tplants.2015.06.008.
- 662 **Kim D, Langmead B, Salzberg SL. 2015.** HISAT: A fast spliced aligner with low memory
663 requirements. *Nature Methods* **12**:357–360. DOI 10.1038/nmeth.3317.
- 664 **Kim JH, Nguyen NH, Jeong CY, Nguyen NT, Hong SW, Lee H. 2013.** Loss of the R2r3 Myb,
665 Atmyb73, causes hyper-induction of the *Sos1* and *Sos3* genes in response to high salinity in
666 *Arabidopsis*. *Journal of Plant Physiology* **170(16)**:1461–1465 DOI 10.1016/j.jplph.2013.05.011.
- 667 **Kumar P, Sharma PK. 2020.** Soil salinity and food security in India. *Frontiers in Sustainable*
668 *Food Systems* **4**:533781 DOI 10.3389/fsufs.2020.533781.
- 669 **Lee J, Lee I. 2010.** Regulation and function of SOC1, a flowering pathway integrator. *Journal of*
670 *Experimental Botany* **61(9)**:2247–2254. DOI 10.1093/jxb/erq098.
- 671 **Lichtenthaler HK. 1987.** Chlorophyll and carotenoids: Pigments of photosynthetic
672 biomembranes. *Methods in Enzymology* **148**:350–382 DOI 10.1016/0076-6879(87)48036-1.
- 673 **Li H, Xu G, Yang C, Yang L, Liang Z. 2019.** Genome-wide identification and expression
674 analysis of HKT transcription factor under salt stress in nine plant species. *Ecotoxicology and*
675 *Environmental Safety* **171**:435–442 DOI 10.1016/j.ecoenv.2019.01.008.
- 676 **Li J, Zhu L, Hull J J, Liang S, Daniell, H Jin S, Zhang X. 2016.** Transcriptome analysis reveals
677 a comprehensive insect resistance response mechanism in cotton to infestation by the phloem
678 feeding insect *Bemisia tabaci* (whitefly). *Plant Biotechnology Journal* **14(10)**:1956–1975 DOI
679 10.1111/pbi.12554.
- 680 **Li J, Wang T, Han J, Ren Z. 2020a.** Genome-wide identification and characterization of
681 cucumber bHLH family genes and the functional characterization of CsbHLH041 in NaCl and
682 ABA tolerance in *Arabidopsis* and cucumber. *BMC Plant Biology* **20**:1–20 DOI 10.1186/s12870-
683 020-02440-1.
- 684 **Li WY, Wang C, Shi HH, Wang B, Wang J. X, Liu YS, Ma JY, Tian SY, Zhang YW. 2020b.**
685 Genome-wide analysis of ethylene-response factor family in adzuki Bean and functional
686 determination of Vaerf3 under saline-alkaline stress. *Plant Physiology and Biochemistry* **147**:215–
687 222 DOI 10.1016/j.plaphy.2019.12.019.
- 688 **Lloyd A, Brockman A, Aguirre L, Campbell A, Bean A, Cantero A, Gonzalez A. 2017.**
689 Advances in the Myb–bHLH–Wd repeat (MBW) pigment regulatory model: Addition of a Wrky

- 690 factor and Co-option of an anthocyanin Myb for betalain regulation. *Plant & Cell Physiology*
691 **58(9)**:1431–1441. DOI: 10.1093/pcp/pcx075
- 692 **Long W, Zou X, Zhang X. 2015.** Transcriptome analysis of canola (*Brassica napus*) under salt
693 stress at the germination stage. *PLOS ONE* **10(2)**:e0116217. DOI 10.1371/journal.pone.0116217
- 694 **Luo H, Huo P, Wang Z, Zhang S, He Z, Wu Y, Zhao L, Liu J, Guo J, Fang S, Cao W, Yi L,**
695 **Zhao Y, Kong L. 2021.** KOBAS-i: Intelligent prioritization and exploratory visualization of
696 biological functions for gene enrichment analysis. *Nucleic Acids Research* **49(W1)**:W317–W325.
697 DOI 10.1093/nar/gkab447
- 698 **Merico D, Isserlin R, Stueker O, Emili A, Bader GD. 2010.** Enrichment map: A network-based method
699 for gene-set enrichment visualization and interpretation. *PLOS ONE* **5(11)**:e13984 DOI
700 10.1371/journal.pone.0013984
- 701 **Møller IS, Tester M. 2007.** Salinity tolerance of *Arabidopsis*: A good model for cereals? *Trends*
702 *in Plant Science* **12(12)**:534–540 DOI 10.1016/j.tplants.2007.09.009.
- 703 **Møller IS, Gilliam M, Jha D, Mayo GM, Roy SJ, Coates JC, Haseloff J, Tester M. 2009.**
704 Shoot Na⁺ exclusion and increased salinity tolerance engineered by cell type-specific alteration of
705 Na⁺ transport in *Arabidopsis*. *Plant Cell* **21(7)**:2163–2178 DOI 10.1105/tpc.108.064568.
- 706 **Munns R, James RA, Xu B, Athman A, Conn SJ., Jordans C, Byrt CS, Hare RA, Tyerman**
707 **SD, Tester M, Plett D, Gilliam M. 2012.** Wheat grain yield on saline soils is improved by an
708 ancestral Na⁺ transporter gene. *Nature Biotechnology* **30**:360–364 DOI 10.1038/nbt.2120.
- 709 **Munns R, Tester M. 2008.** Mechanisms of salinity tolerance. *Annual Review of Plant Biology*
710 **59**:651–681 DOI 10.1146/annurev.arplant.59.032607.092911.
- 711 **Naeem M, Iqbal M, Shakeel A, Ul-Allah S, Hussain M, Rehman A, Zafar ZU, Athar HuR,**
712 **Ashraf M. 2020.** Genetic basis of ion exclusion in salinity stressed wheat: implications in
713 improving crop yield. *Plant Growth Regulation* **92**:479–496 DOI 10.1007/s10725-020-00659-4.
- 714 **Nguyen NH, Cheong JJ. 2018.** H2A.Z-containing nucleosomes are evicted to activate AtMYB44
715 transcription in response to salt stress. *Biochemical Biophysical Research Communications*
716 **499(4)**:1039–1043 DOI 10.1016/j.bbrc.2018.04.048.
- 717 **Nakano T, Suzuki K, Fujimura T, Shinshi H. 2006.** Genome-wide analysis of the ERF gene
718 family in *Arabidopsis* and rice. *Plant Physiology* **140(2)**:411–432 DOI: 10.1104/pp.105.073783.
- 719 **Nieves-Cordones M, Al Shiblawi FR, Sentenac H. 2016.** Roles and transport of sodium and
720 potassium in plants. *Metal Ions in Life Sciences* **16**:291–324 DOI 10.1007/978-3-319-21756-7_9.
- 721 **Omran S, Arzani A, Esmailzadeh Moghaddam ME, Mahlooji M. 2022.** Genetic analysis of
722 salinity tolerance in wheat (*Triticum aestivum* L.). *PLOS ONE* **17(3)**:e0265520 DOI
723 10.1371/journal.pone.0265520.
- 724 **Oliveira DM, Mota TR, Salatta FV, Sinzker RC, Končítiková R, Kopečný D, Dos Santos WD.**
725 **2020.** Cell wall remodeling under salt stress: Insights into changes in polysaccharides,
726 feruloylation, lignification, and phenolic metabolism in maize. *Plant Cell & Environment* **43(9)**:
727 2172–2191 DOI: 10.1111/pce.13805

- 728 **Peng Z, He S, Gong W, Sun J, Pan Z, Xu F, Lu Y, Du X. 2014.** Comprehensive analysis of
729 differentially expressed genes and transcriptional regulation induced by salt stress in two
730 contrasting cotton genotypes. *BMC Genomics* **15**:1–28 DOI 10.1186/1471-2164-15-760.
- 731 **Raudvere U, Kolberg L, Kuzmin I, Arak T, Adler P, Peterson H, Vilo JG. 2019.** g:Profiler: A web
732 server for functional enrichment analysis and conversions of gene lists (2019 update). *Nucleic Acids*
733 *Research* **47(W1)**:W191–W198 DOI: 10.1093/nar/gkz369.
- 734 **Riedelsberger J, Miller JK, Valdebenito-Maturana B, Piñeros MA, González W, Dreyer I.**
735 **2021.** Plant HKT channels: An updated view on structure, function and gene regulation.
736 *International Journal of Molecular Sciences* **22(4)**:1892 DOI 10.3390/ijms22041892.
- 737 **Robinson MD, McCarthy DJ, Smyth GK. 2010.** Edger: A bioconductor package for differential
738 expression analysis of digital gene expression data. *Bioinformatics* **26(1)**:139–140 DOI
739 10.1093/bioinformatics/btp616.
- 740 **Saade S, Brien C, Pailles Y, Berger B, Shahid M, Russell J, Waugh R, Negrão S, Tester M.**
741 **2020.** Dissecting new genetic components of salinity tolerance in two-row spring barley at the
742 vegetative and reproductive stages. *PLOS ONE* **15(7)**:e0236037 DOI
743 10.1371/journal.pone.0236037.
- 744 **Sadak M S. 2019.** Physiological role of trehalose on enhancing salinity tolerance of wheat plant.
745 *Bulletin of National Research Centre* **43**:1–10 DOI: 10.1186/s42269-019-0098-6.
- 746 **Sayed HI. 1985.** Diversity of salt tolerance in a germplasm collection of wheat (*Triticum* spp.).
747 *Theoretical and Applied Genetics* **69**:651–657 DOI 10.1007/BF00251118.
- 748 **Schachtman DP, Schroeder JI. 1994.** Structure and transport mechanism of a high-affinity
749 potassium uptake transporter from higher plants. *Nature* **370(6491)**:655–658 DOI
750 10.1038/370655a0.
- 751 **Seleiman M, Talha Aslam M, Ahmed Alhammad B, Umair Hassan M, Maqbool R, Umer**
752 **Chattha M, Khan I, Ireri Gitari H, S Uslu O, Roy R, Leonardo Battaglia M. 2022.** Salinity
753 Stress in Wheat: Effects, Mechanisms and Management Strategies. *Phyton-International Journal*
754 *of Experimental Botany* **91(4)**:667–694 DOI: 10.32604/phyton.2022.017365.
- 755 **Seo JS, Sohn HB, Noh K, Jung C, An JH, Donovan CM, Somers DA, Kim DI, Jeong SC, Kim**
756 **CG, Kim HM, Lee S, Choi YD, Moon TW, Kim CH, Cheong J. 2012.** Expression of the
757 Arabidopsis Atmyb44 gene confers drought/salt-stress tolerance in transgenic soybean. *Molecular*
758 *Breeding* **29**:601–608 DOI 10.1007/s11032-011-9576-8.
- 759 **Shavrukov Y, Langridge P, Tester M. 2009.** Salinity tolerance and sodium exclusion in genus
760 *Triticum*. *Breeding Science* **59(5)**:671–678. DOI 10.1270/jsbbs.59.671.
- 761 **Shiferaw B, Smale M, Braun HJ, Duveiller E, Reynolds M, Muricho G. 2013.** Crops that feed
762 the world 10. Past successes and future challenges to the role played by wheat in global food
763 security. *Food Security* **5**:291–317 DOI 10.1007/s12571-013-0263-y.
- 764 **Singh V, Singh A., Bhadoria J, Giri J, Singh J, TV V, Sharma, PC. 2018.** Differential
765 expression of salt-responsive genes to salinity stress in salt-tolerant and salt-sensitive rice (*Oryza*
766 *sativa* L.) at seedling stage. *Protoplasma* **255**:1667-1681 DOI 10.1007/s00709-018-1257-6

- 767 **Singh DP, Sarkar RK. 2014.** Distinction and characterisation of salinity tolerant and sensitive
768 rice cultivars as probed by the chlorophyll fluorescence characteristics and growth parameters.
769 *Functional Plant Biology* **41(7)**:727–736 DOI 10.1071/FP13229.
- 770 **Sreenivasulu N, Usadel B, Winter A, Radchuk V, Scholz U, Stein N, Weschke W, Strickert M, Close**
771 **TJ, Stitt M, Graner A, Wobus U. 2008.** Barley grain maturation and germination: Metabolic pathway
772 and regulatory network commonalities and differences highlighted by new MapMan/PageMan profiling
773 tools. *Plant Physiology* **146(4)**:1738–1758 DOI 10.1104/pp.107.111781.
- 774 **Subramanian A, Tamayo P, Mootha VK, Mukherjee S, Ebert BL, Gillette MA, Paulovich A, Pomeroy**
775 **SL, Golub TR, Lander ES, Mesirov JP. 2005.** Gene set enrichment analysis: A knowledge-based
776 approach for interpreting genome-wide expression profiles. *Proceedings of the National Academy*
777 *of Sciences* **102(43)**:15545–15550 DOI 10.1073/pnas.0506580102.
- 778 **Tian F, Yang DC, Meng YQ, Jin J, Gao G. 2020.** Plantregmap: Charting functional regulatory
779 maps in plants. *Nucleic Acids Research* **48(D1)**:D1104–D1113 DOI 10.1093/nar/gkz1020.
- 780 **Tohge T, de Souza LP, Fernie AR. 2017.** Current understanding of the pathways of flavonoid
781 biosynthesis in model and crop plants. *Journal of Experimental Botany* **68(15)**:4013–4028 DOI
782 10.1093/jxb/erx177.
- 783 **Trujillo LE, Sotolongo M, Menéndez C, Ochogavía ME, Coll Y, Hernández I, Borrás-**
784 **Hidalgo O, Thomma BP, Vera P, Hernández L. 2008.** Soderf3, a novel sugarcane ethylene
785 responsive factor (erf), enhances salt and drought tolerance when overexpressed in tobacco plants.
786 *Plant & Cell Physiology* **49(4)**:512–525 DOI 10.1093/pcp/pcn025.
- 787 **Tsai YC, Chen KC, Cheng TS, Lee C, Lin SH, Tung CW. 2019.** Chlorophyll fluorescence
788 analysis in diverse rice varieties reveals the positive correlation between the seedlings salt
789 tolerance and photosynthetic efficiency. *BMC Plant Biology* **19**:1–517 DOI 10.1186/s12870-019-
790 1983-8.
- 791 **Vera Alvarez R, Pongor LS, Mariño-Ramírez L, Landsman D. 2019.** TPMCalculator: One-
792 step software to quantify mRNA abundance of genomic features. *Bioinformatics* **35(11)**:1960–
793 1962 DOI 10.1093/bioinformatics/bty896.
- 794 **Wu J, Yu C, Hunag L, Wu M, Liu B, Liu Y, Song G, Liu D, Gan Y. 2020.** Overexpression of
795 MADS-box transcription factor OsMADS25 enhances salt stress tolerance in Rice and
796 Arabidopsis. *Plant Growth Regulation* **90**:163–171 DOI 10.1007/s10725-019-00539-6.
- 797 **Yang Q, Chen ZZ, Zhou X F, Yin HB, Li X, Xin XF, Hong XH, Zhu JK, Gong Z. 2009.**
798 Overexpression of SOS (salt overly sensitive) genes increases salt tolerance in transgenic
799 Arabidopsis. *Molecular Plant* **2(1)**:22–31 DOI 10.1093/mp/ssn058.
- 800 **Yang YY, Zheng PF, Ren YR, Yao YX, You CX, Wang XF, Hao YJ. 2021.** Apple Mdsat1
801 encodes a bHLHm1 transcription factor involved in salinity and drought responses. *Planta* **253**:46
802 1–13 DOI 10.1007/s00425-020-03528-6.
- 803 **Yuan YW, Sagawa JM, Frost L, Vela JP, Bradshaw HD Jr. 2014.** Transcriptional control of
804 floral anthocyanin pigmentation in monkeyflowers (*Mimulus*). *New Phytologist* **204(4)**:1013–
805 1027 DOI 10.1111/nph.12968.

- 806 **Zhang, S., Chen, C., Li, L., Meng, L., Singh, J., Jiang, N., & Lemaux, P. G. 2005.** Evolutionary
807 expansion, gene structure, and expression of the rice wall-associated kinase gene family. *Plant*
808 *Physiology* **139(3)**:1107-1124 DOI 10.1104/pp.105.069005.
- 809 **Zhang Y, Fang J, Wu X. Na Dong L 2018.** Na⁺/K⁺ balance and transport Regulatory mechanisms
810 in weedy and cultivated rice (*Oryza sativa* L.) under salt stress. *BMC Plant Biology* **18**:1–14 DOI
811 10.1186/s12870-018-1586-9.
- 812 **Zhao PX, Zhang J, Chen SY, Wu J, Xia JQ, Sun LQ, Ma SS, Xiang CB. 2021.** Arabidopsis
813 MADS-box factor AGL16 is a negative regulator of plant response to salt stress by downregulating
814 salt-responsive genes. *New Phytologist* **232(6)**:2418–2439 DOI 10.1111/nph.17760.
- 815 **Zheng J, Wu H, Zhu H, Huang C, Liu C, Chang Y, Kong Z, Zhou Z, Wang G, Lin Y, Chen**
816 **H. 2019.** Determining factors, regulation system, and domestication of anthocyanin biosynthesis
817 in rice leaves. *New Phytologist* **223(2)**:705–721 DOI 10.1111/nph.15807.
- 818

819 **Figure titles and legends**

820 **Figure 1. Effect of salt stress on seed germination and seedling growth.**

821 (A) Germination rate of wheat seeds under different salt concentrations. 500 seeds from each line
822 were placed on two layers of germination paper and exposed to a solution containing 150mM NaCl
823 in a phytohealth chamber (SPL Life Sciences) at a temperature of 22°C. Germination was assessed
824 after 4 days. (B) Wheat seedling growth under different salinity levels. Seven-day-old seedlings
825 were subjected to a salt stress treatment with a total volume of 200ml of the solution containing
826 150mM NaCl after 4 days. (C) Phenotypes of wheat seedlings under different salinity levels after
827 4 days of salt stress with a total volume of 200ml of the solution containing 150mM NaCl. (D)
828 Shoot and root lengths of wheat seedlings under different salinity conditions after 4 days of salt
829 stress with a total volume of 200ml of the solution containing 150mM NaCl. Independent t-tests
830 demonstrated significant differences (* $p < 0.05$ and ** $p < 0.01$).

831

832 **Figure 2. Na⁺ and K⁺ ion contents, differential ratios of K⁺ and Na⁺ and chlorophyll** 833 **concentrations for PL1 and PL6 under salt stress treatment.**

834 Seven-day-old seedlings were subjected to a salt stress treatment with a total volume of 200ml of
835 the solution containing 150mM NaCl. After treatment with 150 mM NaCl, wheat leaves were
836 collected at 0, 3, 24, and 48 hours. (A) Na⁺ ion content in the shoots under different salt stress
837 exposure times. (B) K⁺ ion content in the shoots under different salt stress exposure times. (C)
838 Changes in the relative "Na⁺ ratio" in shoots at different time points after salt stress treatment. The
839 "Na⁺ ratio" represents the relative proportion of Na⁺ content in shoots compared to the Na⁺ content
840 at 0 hours (baseline). Data points at 3 hours, 24 hours, and 48 hours indicate the fold change of
841 Na⁺ content in shoots compared to the baseline (0 hours). (D) Changes in the relative "K⁺ ratio"
842 in shoots at different time points after salt stress treatment. The "K⁺ ratio" represents the relative
843 proportion of K⁺ content in shoots compared to the K⁺ content at 0 hours (baseline). Data points
844 at 3 hours, 24 hours, and 48 hours indicate the fold change of K⁺ content in shoots compared to
845 the baseline (0 hours). (E) Chlorophyll concentrations in the shoots under different salt stress
846 exposure times. Each bar represents the mean ± standard error (n = 3). Independent t-tests showed
847 significant differences (* $p < 0.05$ and ** $p < 0.01$).

848

849 **Figure 3. Differentially expressed genes (DEGs) and Gene Set Enrichment Analysis (GSEA)** 850 **for PL1 and PL6.**

851 (A) Venn diagrams showing the number of DEGs between PL1 and PL6 and the overlap of all
852 DEGs at different time points after exposure to salt stress. (B) Number of DEGs only expressed in
853 PL1 at different time points after exposure to salt stress. (C) Number of DEGs only expressed in
854 PL6 at different time points after exposure to salt stress. (D) GSEA enrichment analysis with gene
855 ontology of the DEGs. Dots indicate significant GO terms from the pairwise gene set enrichment
856 analysis comparisons at each time point after exposure to salt stress. The size of the dots indicates
857 the number of genes, and the color of the dots indicates the $-\log_{10}$ FDR value within the pathway.

858

859 **Figure 4. Gene ontology (GO) Enrichment Map and differential gene expression profiling** 860 **for PL1 and PL6.**

861 (A–E) Five networks of significantly enriched gene sets between PL1 and PL6 obtained on the
862 Enrichment Map. Nodes representing enriched gene sets were classified based on their similarity
863 to related gene sets. The size of the node is proportional to the total number of genes. The thickness
864 of the green line between nodes represents the proportion of shared genes between gene sets. (F–

865 J) The expression patterns of each network at each time point after exposure to salt stress. Each
866 cluster represents a group of functionally related gene sets that showed similar expression patterns.
867 Figure 4F, 4G, 4H, 4I, and 4J show multiple clusters derived from the networks of Figures 4A,
868 4B, 4C, 4D, and 4E, respectively. Clusters showing different expression patterns between PL1 and
869 PL6 were indicated in red boxes. (K) Heatmaps representing the expressions of differentially
870 expressed genes (DEGs) marked in red boxes (F, G, and I) for PL1 and PL6.

871

872 **Figure 5. Gene Set Enrichment Analysis with Kyoto Encyclopedia of Genes and Genomes**
873 **(KEGG) pathways of the differentially expressed genes (DEGs).**

874 Dots represent significant KEGG pathways from the pairwise gene set enrichment analysis
875 comparisons at each time point after exposure to salt stress. The size of the dots indicates the
876 number of differential genes, while the color of the dots represents the p-values of enrichment
877 analysis. The rich factor refers to the ratio of the number of DEGs in the pathway to the total
878 number of genes. The size of the dots indicates the number of genes, and the color of the dots
879 indicates the $-\log_{10}$ FDR value within the pathway.

880

881 **Figure 6. Differentially expressed transcription factors (TFs) under salt stress treatment in**
882 **PL1 and PL6.**

883 (A) Distribution of TF family members among the differentially expressed genes (DEGs). The bar
884 graph illustrates the number of TFs belonging to each TF family among the DEGs. (B) Expression
885 patterns of TFs at each time point after exposure to salt stress. Each cluster with similar expression
886 patterns is indicated by red boxes. (C) Heatmap analysis of TF family genes in PL1 and PL6 under
887 salt stress treatment, with the genes marked by red boxes in (B) specifically highlighted.

888

889 **Figure 7. Biochemical assays of antioxidant enzyme activity.**

890 (A) Catalase (CAT) activity, (B) Peroxidase (POD) activity, (C) Total Superoxide Dismutase
891 (SOD) activity, and (D) Total Antioxidant Capacity (TAC). Each bar represents the average \pm
892 standard error ($n = 3$). Independent t-tests demonstrated significant differences ($* p < 0.05$ and $**$
893 $p < 0.01$) compared to the control condition (0h).

894

895 **Figure 8. Validation of the RNA sequencing results via reverse transcription-quantitative**
896 **polymerase chain reaction (RT-qPCR) at different timepoints under salt stress conditions.**

897 Three clusters representing different expression patterns for PL1 and PL6 were selected and the
898 relative expressions shown. RT-qPCR was performed with three biological replicates. Each bar
899 represents the average \pm standard error ($n = 3$). Independent t-tests showed significant differences
900 ($* p < 0.05$ and $** p < 0.01$)

901

902 **Supplemental information Titles and Legends**

903 **Supplementary Figure 1 (Fig. S1). Field images of M6 generations of PL1 and PL6 at**
904 **different time points.**

905 (A) Plot images of M6 generations of PL1 and PL6 at different time points. (B) and (C) Different
906 views of the field at various time points. The dates when the photos were taken are indicated below
907 each image.

908

909 **Supplementary Figure 2 (Fig. S2). Comparison of seed coat color of different wheat lines.**

910 PL1 (control) and PL6 (mutant lines) were used in this study.

911

912 **Supplementary Figure 3 (Fig. S3). Comparison of salt stress response in mutant lines (PL2-**
913 **PL49) and wild type control (PL1).**

914 (A) Germination rate of mutant lines (PL2-PL49) and PL1 as the wild type control. (B) Shoot
915 length of mutant lines (PL2-PL49) and PL1 as the wild type control. (C) Root length of mutant
916 lines (PL2-PL49) and PL1 as the wild type control. For the preliminary screening of the selected
917 mutant lines, 100 seeds from each line were placed in a phytohealth chamber (SPL Life Sciences)
918 with two layers of germination paper, and a total volume of 200ml of the solution containing
919 150mM NaCl was applied to them at a temperature of 22°C. After 4 days, the germination rate,
920 shoot length, and root length were recorded. PL1 served as the wild type control in these
921 experiments.

922

923 **Supplementary Table 1 (Table S1). The details of the primers used in this study.**

924

925 **Supplementary Table 2 (Table S2). Germination ratio the different salt concentrations on**
926 **seed germination.**

927

928 **Supplementary Table 3 (Table S3). Summary of RNA-seq quality, read counts, and mapping**
929 **rates.**

930

931 **Supplementary Table 4 (Table S4). Differentially expressed genes (DEGs) from BlastX**
932 **results against NCBI Poaceae family.**

933 This table contains the blastx results against the NCBI *Poaceae* family, which led to the
934 identification of a total of 4,017 differentially expressed genes (DEGs) with a p-value < 0.05 and
935 FDR < 0.05.

936

937 **Supplementary Table 5 (Table S5). Gene Set Enrichment Analysis (GSEA) for PL1 and PL6**
938 **using gene ontology (GO) mapping of differentially expressed genes.**

939

940 **Supplementary Table 6 (Table S6). Gene Set Enrichment Analysis (GSEA) for PL1 and PL6**
941 **using Kyoto Encyclopedia of Genes and Genomes (KEGG) pathways mapping of**
942 **differentially expressed genes.**

943

944 **Supplementary Table 7 (Table S7). Differentially express genes in red boxes of Fig. 6B used**
945 **in Fig. 6C.**

946

Figure 1

Figure 1. Effect of salt stress on seed germination and seedling growth.

(A) Germination rate of wheat seeds under different salt concentrations. 500 seeds from each line were placed on two layers of germination paper and exposed to a solution containing 150mM NaCl in a phytohealth chamber (SPL Life Sciences) at a temperature of 22°C. Germination was assessed after 4 days. (B) Wheat seedling growth under different salinity levels. Seven-day-old seedlings were subjected to a salt stress treatment with a total volume of 200ml of the solution containing 150mM NaCl after 4 days. (C) Phenotypes of wheat seedlings under different salinity levels after 4 days of salt stress with a total volume of 200ml of the solution containing 150mM NaCl. (D) Shoot and root lengths of wheat seedlings under different salinity conditions after 4 days of salt stress with a total volume of 200ml of the solution containing 150mM NaCl. Independent t-tests demonstrated significant differences (* $p < 0.05$ and ** $p < 0.01$).

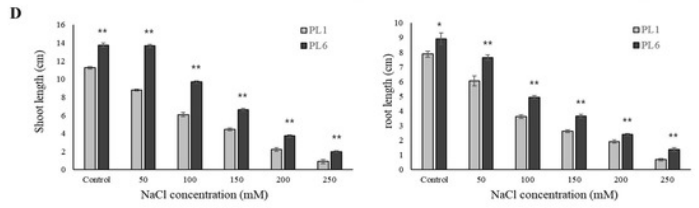
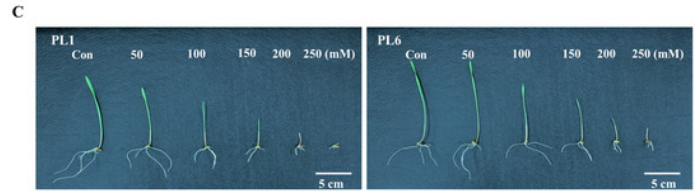
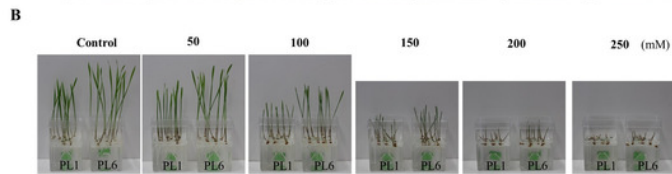
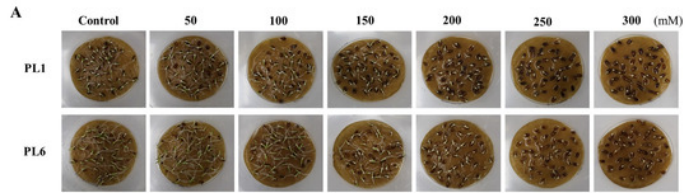


Figure 2

Figure 2. Na⁺ and K⁺ ion contents, differential ratios of K⁺ and Na⁺ and chlorophyll concentrations for PL1 and PL6 under salt stress treatment.

Seven-day-old seedlings were subjected to a salt stress treatment with a total volume of 200ml of the solution containing 150mM NaCl. After treatment with 150 mM NaCl, wheat leaves were collected at 3, 24, and 48 hours. (A) Na⁺ ion content in the shoots under different salt stress exposure times. (B) K⁺ ion content in the shoots under different salt stress exposure times. (C) Changes in the relative "Na⁺ ratio" in shoots at different time points after salt stress treatment. The "Na⁺ ratio" represents the relative proportion of Na⁺ content in shoots compared to the Na⁺ content at 0 hours (baseline). Data points at 3 hours, 24 hours, and 48 hours indicate the fold change of Na⁺ content in shoots compared to the baseline (0 hours). (D) Changes in the relative "K⁺ ratio" in shoots at different time points after salt stress treatment. The "K⁺ ratio" represents the relative proportion of K⁺ content in shoots compared to the K⁺ content at 0 hours (baseline). Data points at 3 hours, 24 hours, and 48 hours indicate the fold change of K⁺ content in shoots compared to the baseline (0 hours). (E) Chlorophyll concentrations in the shoots under different salt stress exposure times. Each bar represents the mean \pm standard error (n = 3). Independent t-tests showed significant differences (* $p < 0.05$ and ** $p < 0.01$).

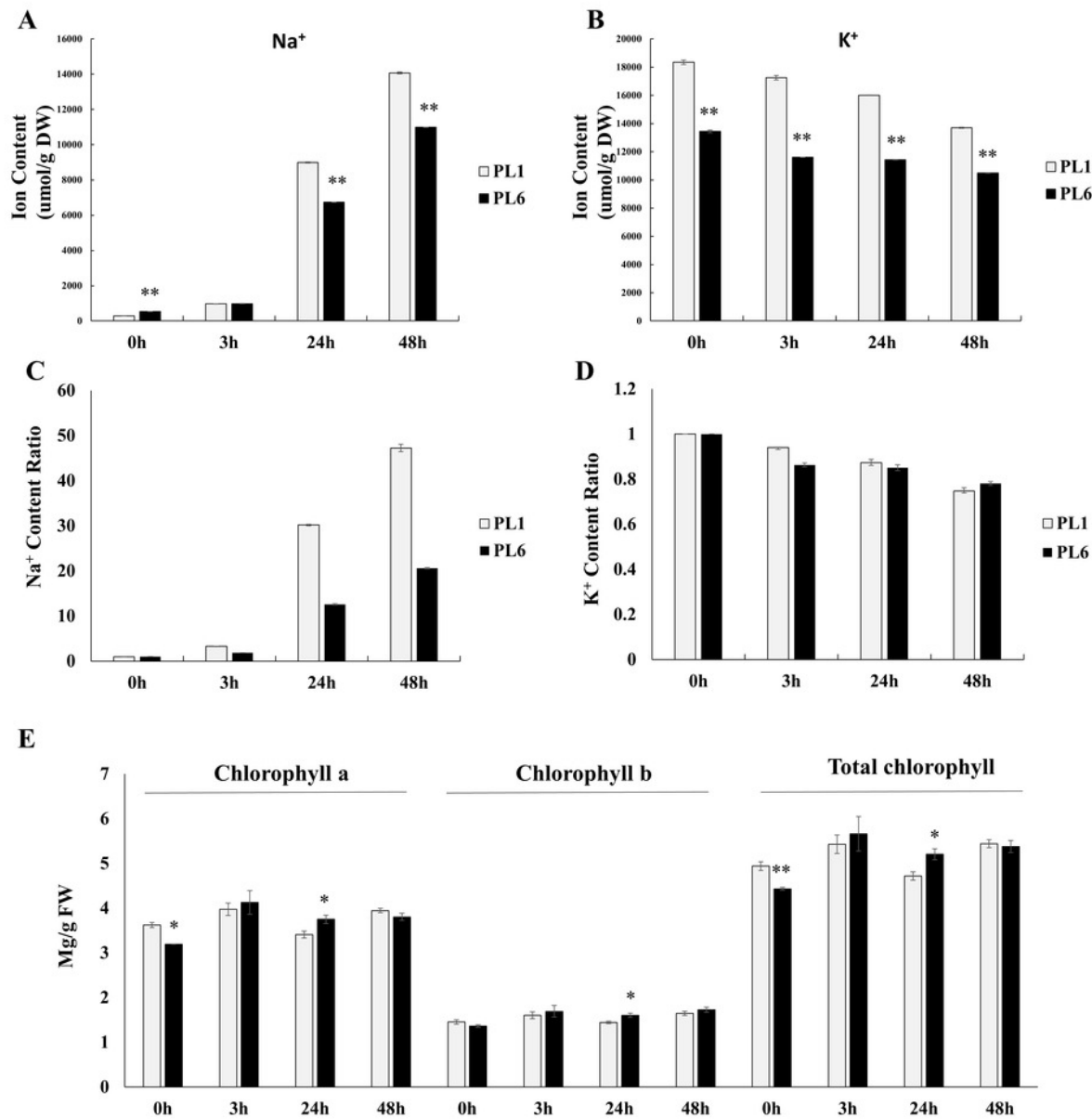


Figure 3

Figure 3. Differentially expressed genes (DEGs) and Gene Set Enrichment Analysis (GSEA) for PL1 and PL6.

(A) Venn diagrams showing the number of DEGs between PL1 and PL6 and the overlap of all DEGs at different time points after exposure to salt stress. (B) Number of DEGs only expressed in PL1 at different time points after exposure to salt stress. (C) Number of DEGs only expressed in PL6 at different time points after exposure to salt stress. (D) GSEA enrichment analysis with gene ontology of the DEGs. Dots indicate significant GO terms from the pairwise gene set enrichment analysis comparisons at each time point after exposure to salt stress. The size of the dots indicates the number of genes, and the color of the dots indicates the $-\log_{10}$ FDR value within the pathway.

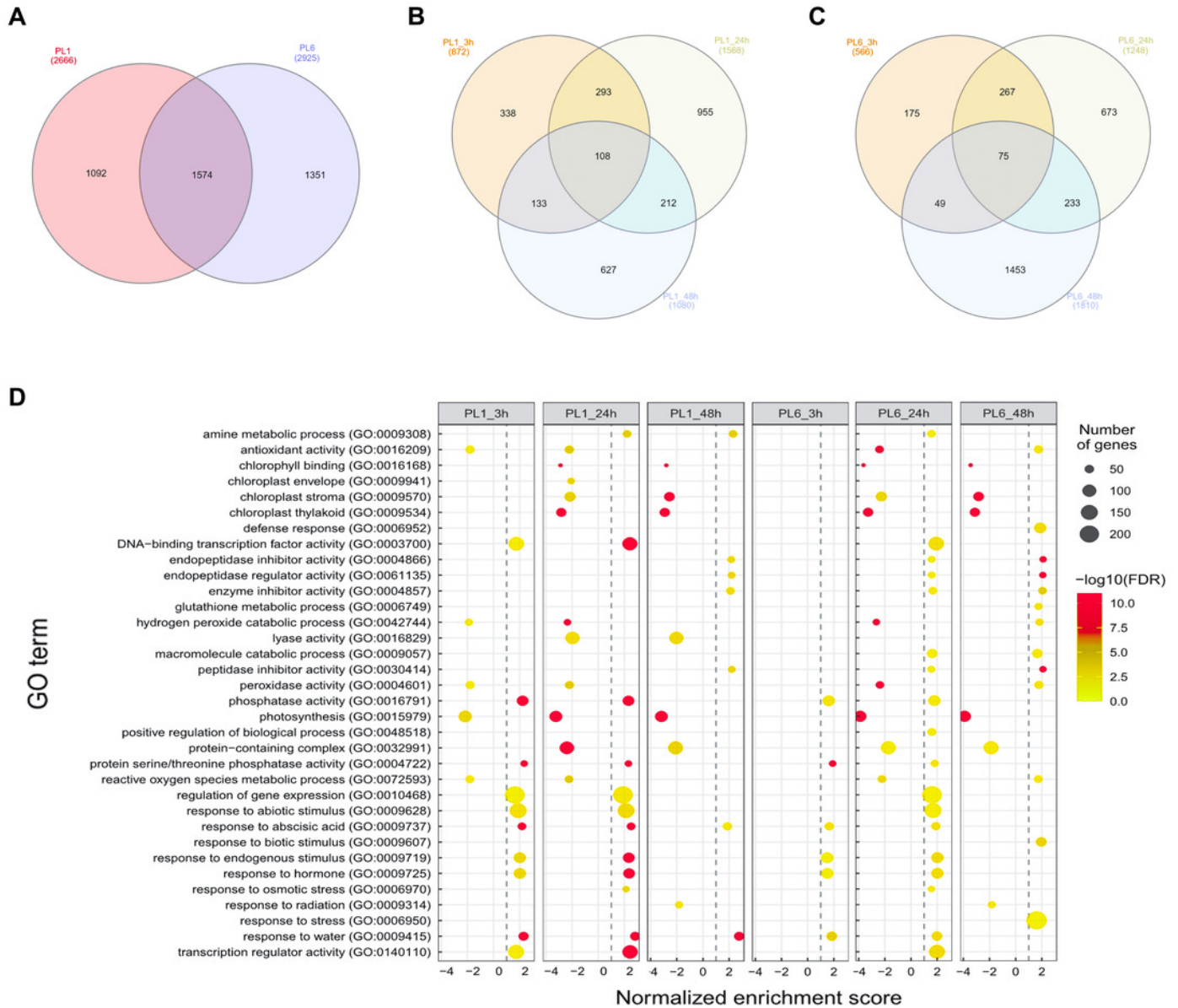


Figure 4

Figure 4. Gene ontology (GO) Enrichment Map and differential gene expression profiling for PL1 and PL6.

(A-E) Five networks of significantly enriched gene sets between PL1 and PL6 obtained on the Enrichment Map. Nodes representing enriched gene sets were classified based on their similarity to related gene sets. The size of the node is proportional to the total number of genes. The thickness of the green line between nodes represents the proportion of shared genes between gene sets. (F-J) The expression patterns of each network at each time point after exposure to salt stress. Each cluster represents a group of functionally related gene sets that showed similar expression patterns. Figure 4F, 4G, 4H, 4I, and 4J show multiple clusters derived from the networks of Figures 4A, 4B, 4C, 4D, and 4E, respectively. Clusters showing different expression patterns between PL1 and PL6 were indicated in red boxes. (K) Heatmaps representing the expressions of differentially expressed genes (DEGs) marked in red boxes (F, G, and I) for PL1 and PL6.

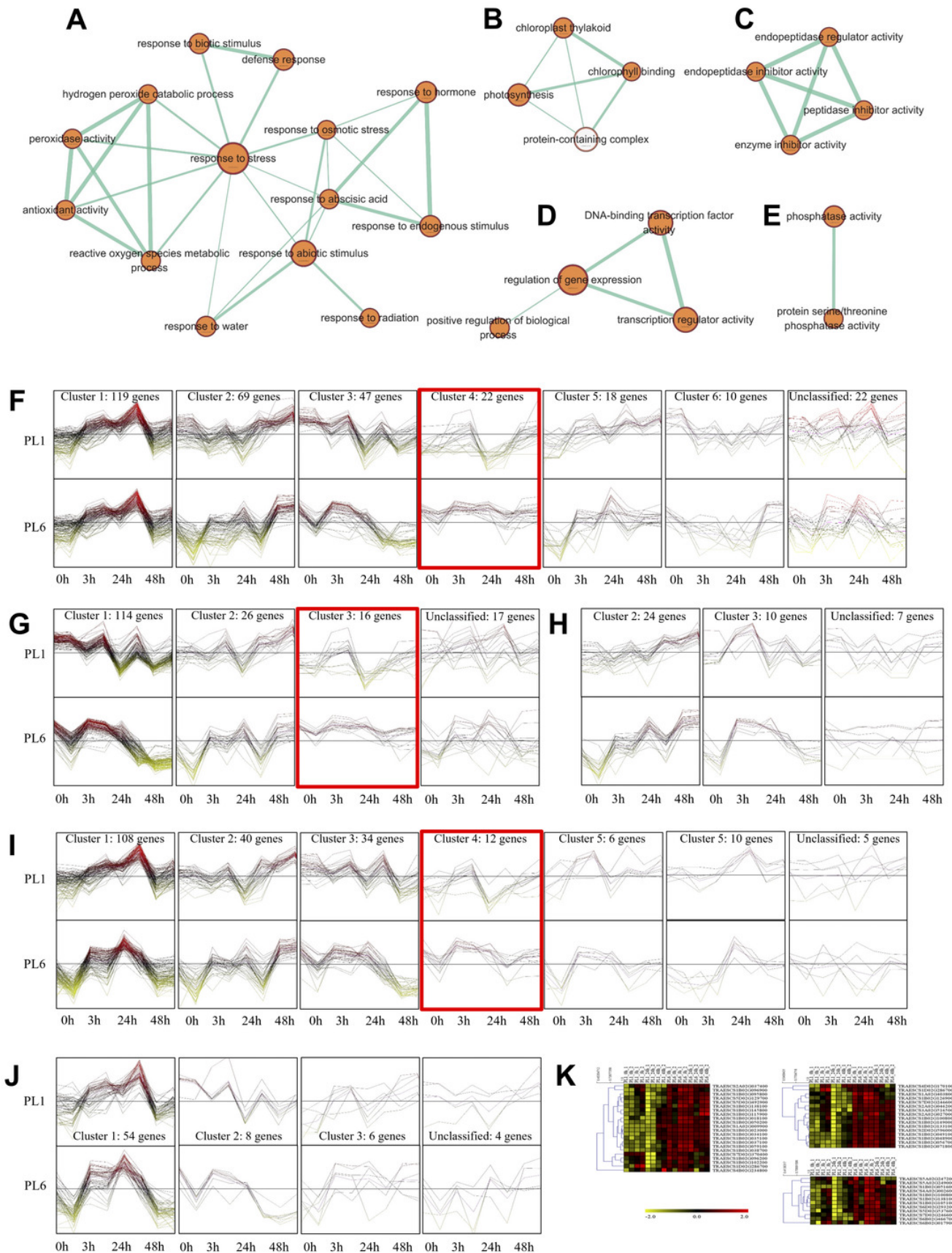


Figure 5

Figure 5. Gene Set Enrichment Analysis with Kyoto Encyclopedia of Genes and Genomes (KEGG) pathways of the differentially expressed genes (DEGs).

Dots represent significant KEGG pathways from the pairwise gene set enrichment analysis comparisons at each time point after exposure to salt stress. The size of the dots indicates the number of differential genes, while the color of the dots represents the p-values of enrichment analysis. The rich factor refers to the ratio of the number of DEGs in the pathway to the total number of genes. The size of the dots indicates the number of genes, and the color of the dots indicates the $-\log_{10}$ FDR value within the pathway.

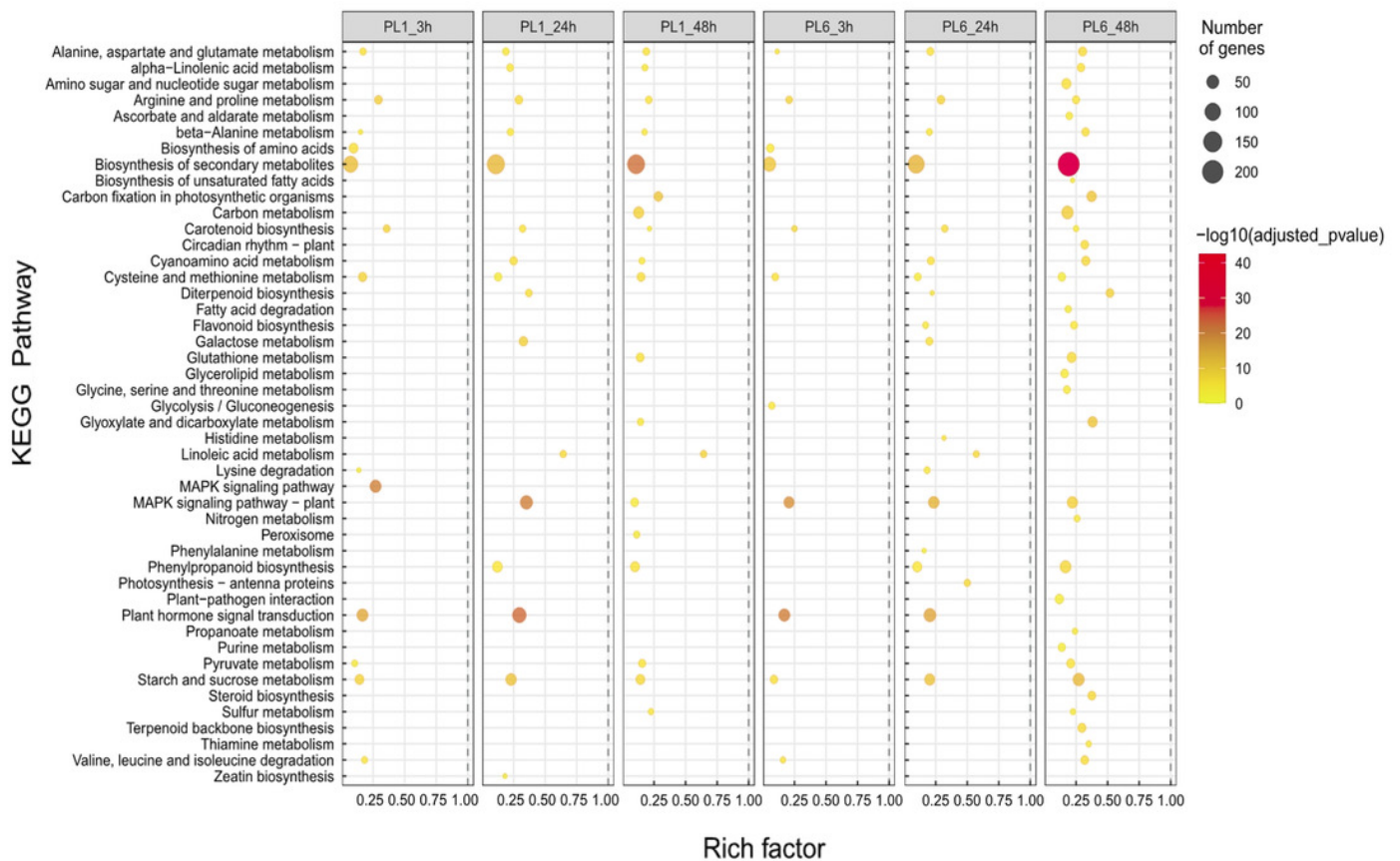
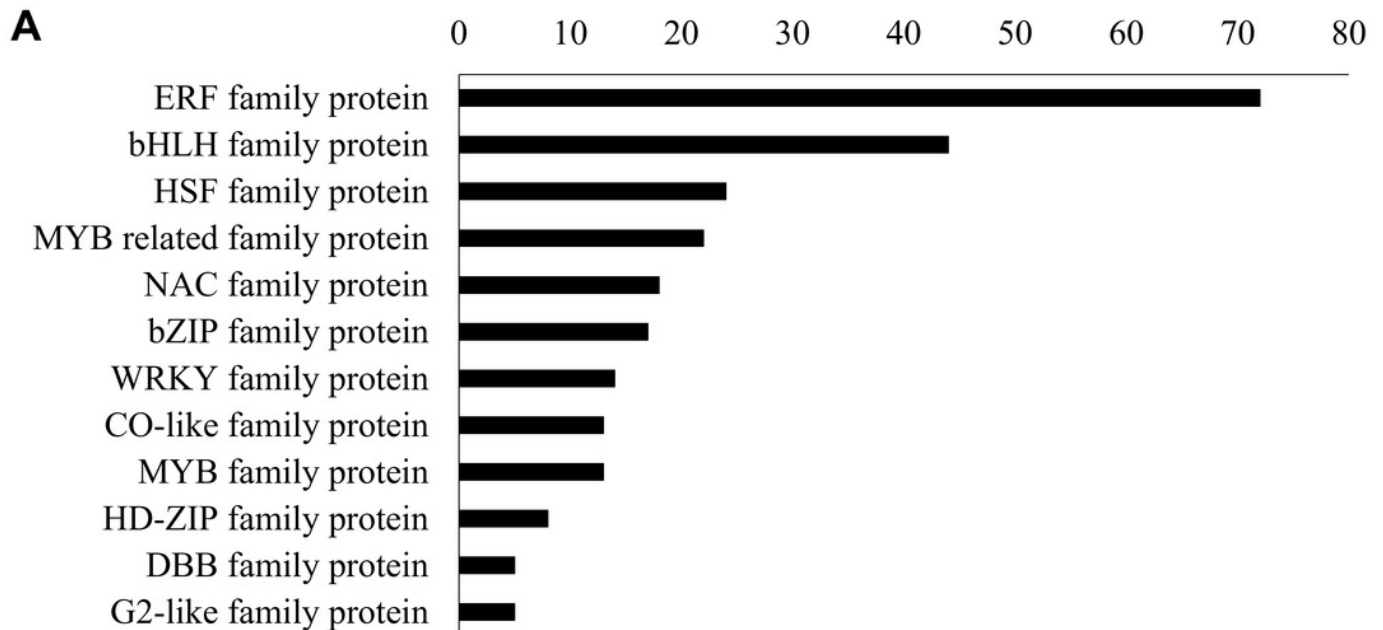


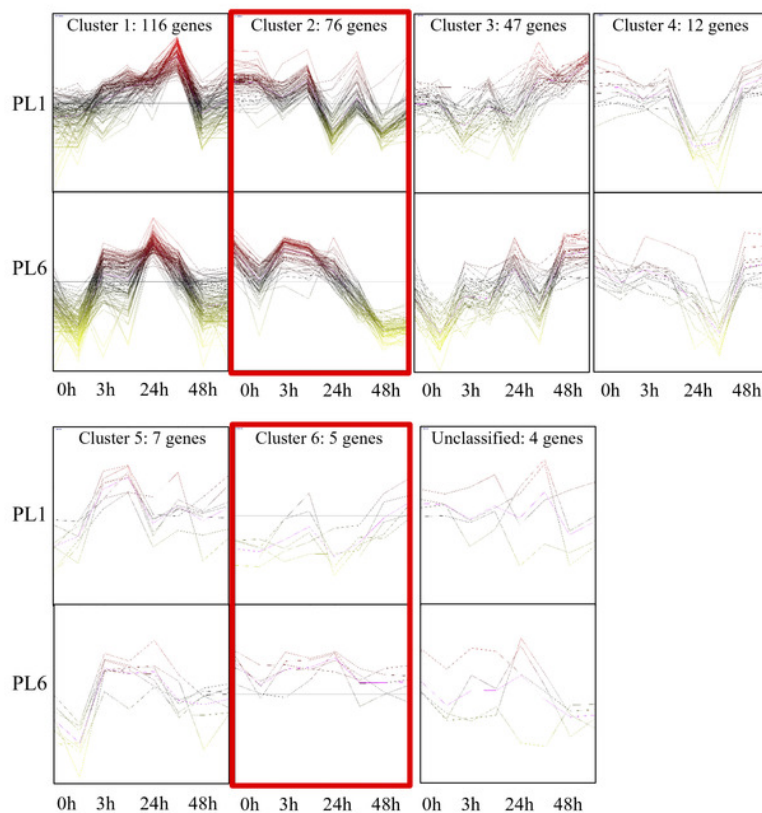
Figure 6

Figure 6. Differentially expressed transcription factors (TFs) under salt stress treatment in PL1 and PL6.

(A) Distribution of TF family members among the differentially expressed genes (DEGs). The bar graph illustrates the number of TFs belonging to each TF family among the DEGs. (B) Expression patterns of TFs at each time point after exposure to salt stress. Each cluster with similar expression patterns is indicated by red boxes. (C) Heatmap analysis of TF family genes in PL1 and PL6 under salt stress treatment, with the genes marked by red boxes in (B) specifically highlighted.



B



C

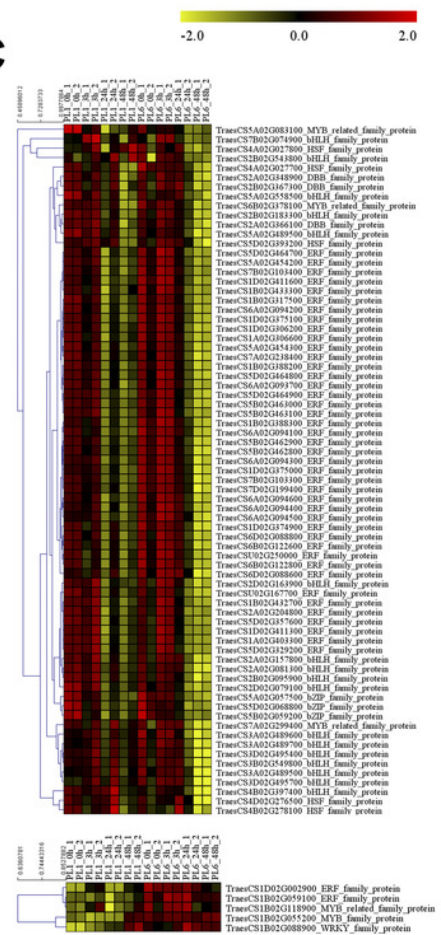


Figure 7

Figure 7. Biochemical assays of antioxidant enzyme activity.

(A) Catalase (CAT) activity, (B) Peroxidase (POD) activity, (C) Total Superoxide Dismutase (SOD) activity, and (D) Total Antioxidant Capacity (TAC). Each bar represents the average \pm standard error ($n = 3$). Independent t-tests demonstrated significant differences (* $p < 0.05$ and ** $p < 0.01$) compared to the control condition (0h).

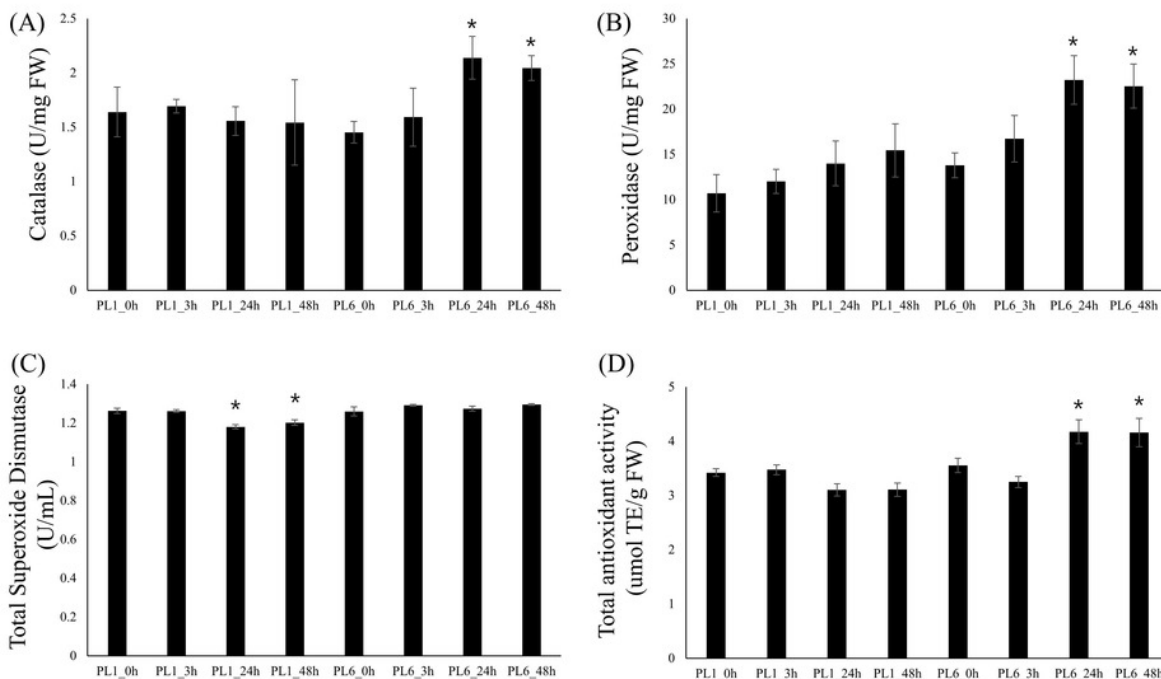


Figure 8

Figure 8. Validation of the RNA sequencing results via reverse transcription-quantitative polymerase chain reaction (RT-qPCR) at different timepoints under salt stress conditions.

Three clusters representing different expression patterns for PL1 and PL6 were selected and the relative expressions shown. RT-qPCR was performed with three biological replicates. Each bar represents the average \pm standard error ($n = 3$). Independent t-tests showed significant differences (* $p < 0.05$ and ** $p < 0.01$)

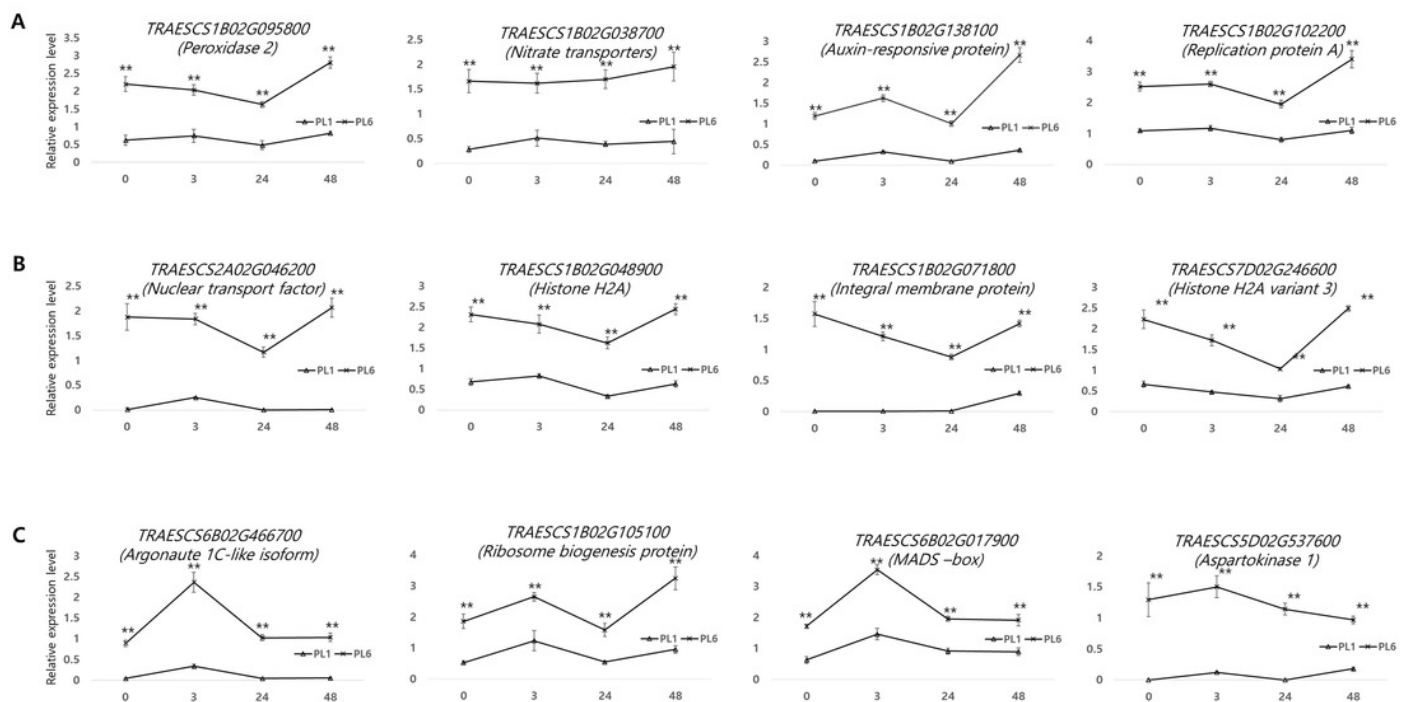


Table 1 (on next page)

Table 1. List of differentially expressed genes selected by K-means clustering from GSEA analysis

1 **Table 1:**2 **List of differentially expressed genes selected by K-means clustering from GSEA analysis.**

Gene ID	Description	Length	E-value	Similarity (%)	Log2 fold change (PL6/PL1)				p-value	FDR	Group
					0 h	3 h	12 h	24 h			
TRAESCS1B02G145800	abscisic acid receptor PYL8	205	1E-149	92.57	4.37	1.96	7.28	1.87	2.09E-19	2.53E-29	
TRAESCS1B02G138100	auxin-responsive protein IAA15	198	2E-143	81.71	3.64	1.88	3.57	2.42	1.56E-28	6.22E-36	
TRAESCS5D02G129700	chaperone protein dnaJ GFA2, mitochondrial	421	0	84.11	8.75	1.57	6.56	5.69	4.77E-38	7.45E-69	
TRAESCS1B02G018100	defensin	81	1.1E-38	84.72	4.86	7.74	5.55	-0.43	1.82E-09	4.81E-93	
TRAESCS1B02G059100	dehydroascorbate reductase	212	9E-156	95.77	3.75	3.64	3.78	1.76	4.05E-69	4.52E-24	DEGs in red boxes
TRAESCS1B02G050200	E3 ubiquitin-protein ligase XB3	486	0	82.96	3.96	3.92	4.48	1.15	1.98E-36	9.28E-17	of cluster 4
TRAESCS5D02G492900	heat shock cognate 70 kDa protein 2	614	0	92.5	3.67	1.74	3.52	3.68	6.04E-97	2.97E-66	in Fig. 4F
TRAESCS1B02G037100	NAD(P)-binding Rossmann-fold superfamily protein	300	0	91.03	5.36	4.72	5.49	2.27	5.67E-67	1.12E-26	
TRAESCS1B02G095800	Peroxidase 2	340	0	89.71	7.85	1.71	7.13	2.85	8.69E-72	9.78E-22	
TRAESCS1B02G096200	peroxidase 5	338	0	85.36	4.99	1.58	4.80	1.88	1.81E-23	3.68E-64	
TRAESCS1B02G096900	Peroxidase 5	343	0	75.36	4.34	1.12	3.82	3.15	7.29E-26	8.91E-18	
TRAESCS1B02G115900	peroxidase A2-like	342	0	82.95	3.84	2.45	4.16	3.27	5.42E-59	3.96E-69	
TRAESCS1B02G038700	protein NRT1/ PTR FAMILY 6.2	582	0	90.52	7.36	8.20	8.09	1.46	1.78E-64	2.32E-34	
TRAESCS1A02G009900	putative disease resistance RPP13-like protein 3	844	0	82.63	6.88	6.49	6.40	-1.81	1.3E-14	2.22E-56	

TRAESCS1B02G023000	putative disease resistance RPP13-like protein 3	920	0	72.15	7.98	8.61	7.67	2.83	2.09E-29	9.97E-62	
TRAESCS1B02G102200	replication protein A 70 kDa DNA-binding subunit C-like	881	0	73.55	4.59	0.95	7.35	2.00	2.3E-18	1.6E-27	
TRAESCS2A02G037400	stress-response A/B barrel domain-containing protein HS1	115	9E-76	85.48	8.11	1.65	8.58	8.10	2.94E-31	2.53E-29	
TRAESCS1B02G034100	subtilisin-chymotrypsin inhibitor CI-1B	74	1.8E-44	84.47	9.97	11.00	11.50	3.89	4.45E-72	3.44E-77	
TRAESCS1B02G035100	subtilisin-chymotrypsin inhibitor CI-1B	74	2.3E-45	84.72	10.70	11.55	12.07	2.56	2.35E-80	4.03E-13	
TRAESCS4D02G170100	60S ribosomal protein L19-1	228	2E-144	88.22	7.03	-0.34	7.73	-7.05	5.65E-47	1.2E-44	
TRAESCS2A02G027000	actin-related protein 9 isoform X1	526	0	84.59	5.48	1.33	3.59	2.19	6.68E-81	1.05E-77	
TRAESCS1B02G133100	DNA-directed RNA polymerases II, IV and V subunit 11	119	2E-86	96.77	8.01	2.08	8.31	2.82	7.37E-23	3.82E-21	
TRAESCS2D02G596000	exocyst complex component EXO70A1	637	0	93.63	6.65	2.49	5.61	2.78	7.27E-83	1.44E-79	DEGs
TRAESCS1B02G048900	histone H2A	154	1E-99	92.72	5.66	5.03	6.05	3.09	2.91E-11	6.97E-10	in red boxes
TRAESCS1B02G049100	histone H2A	155	1E-98	91.26	7.65	8.17	8.49	3.42	4.73E-34	4.76E-32	of cluster 3
TRAESCS1D02G286700	histone H4	103	6.6E-70	99.76	3.41	-1.75	2.65	0.70	6.57E-35	6.97E-33	in Fig. 4G
TRAESCS1B02G149000	INO80 complex subunit D	288	0	82.89	7.67	1.69	7.82	2.84	6.2E-18	3.82E-21	
TRAESCS1B02G126900	NAD(P)H-quinone oxidoreductase subunit S, chloroplastic	239	6E-167	82.95	3.54	1.97	3.25	1.86	3.85E-37	2.43E-16	
TRAESCS2A02G046200	nuclear transport factor 2 (NTF2)-	199	4E-	82.59	8.80	2.01	8.64	8.71	6.74E-30	6.97E-33	

	like protein		115								
TRAESCS1A02G403800	predicted protein	266	0	96.99	2.85	2.44	2.78	1.30	0.006931	1.05E-77	
TRAESCS7D02G370400	predicted protein	312	0	83.35	2.11	-0.21	3.22	2.03	8.65E-36	5.3E-28	
TRAESCS7D02G246600	probable histone H2A variant 3	139	3E-95	95.7	2.08	1.78	3.65	2.75	1.62E-42	1.44E-79	
TRAESCS3A02G516500	Protein COFACTOR ASSEMBLY OF COMPLEX C SUBUNIT B CCB3, chloroplastic	192	4E-117	76.6	7.91	2.26	8.02	8.40	4.51E-69	3.25E-66	
TRAESCS1B02G100800	RNA-binding protein 8A	209	9E-152	85.74	4.77	1.01	4.64	2.08	7.57E-28	1.2E-44	
TRAESCS1B02G071800	thylakoid membrane protein TERC, chloroplastic	377	0	84.39	9.49	8.95	9.08	1.70	3.6E-18	2.67E-40	
TRAESCS1B02G056700	translation initiation factor IF-2 isoform X1	239	7E-174	78.99	6.41	8.58	5.77	2.58	5.67E-56	9.72E-34	
TRAESCS5D02G537600	aspartokinase 1, chloroplastic-like	596	0	68.69	8.62	4.45	9.11	1.84	1.63E-37	2.03E-35	
TRAESCS1B02G138100	auxin-responsive protein IAA15	198	2E-143	81.71	3.64	1.88	3.57	2.42	1.56E-28	1.12E-26	
TRAESCS5A02G247200	glucose-6-phosphate isomerase 1, chloroplastic	614	0	93.86	3.08	1.57	2.09	-0.27	2.07E-28	2.68E-36	DEGs in red boxes
TRAESCS4A02G002600	MADS-box transcription factor 47-like isoform X2	163	7E-116	92.93	3.95	0.66	2.60	3.05	0.000023	0.000247	of cluster 4
TRAESCS7D02G246600	probable histone H2A variant 3	139	3E-95	95.7	2.08	1.78	3.65	2.75	5.65E-47	1.47E-26	in Fig. 4I
TRAESCS6B02G466700	protein argonaute 1C-like isoform X2	1013	0	89.28	5.24	2.58	4.52	5.89	1.53E-64	8.82E-62	
TRAESCS6D02G293200	putative MADS-domain transcription factor	228	1E-167	96.69	5.72	2.42	6.37	2.55	1.46E-42	1.31E-43	
TRAESCS1B02G100800	RNA-binding protein 8A	209	9E-152	85.74	4.77	1.01	4.64	2.08	4.73E-34	2.42E-40	

TRAESCS1B02G105100	ribosome biogenesis protein NOP53	407	0	83.3	4.30	1.07	6.42	2.08	2.01E-38	4.76E-32	<hr/>
TRAESCS1B02G051600	uncharacterized protein LOC109787361	466	0	62.52	6.65	9.45	5.94	3.47	6.62E-46	1.2E-44	

3 **Bold numbers indicate more than two-fold changes in expression.**

Table 2 (on next page)

Table 2. List of diiferentially expressed protein kinase genes under salt stress condition

1 **Table 2:**2 **List of differentially expressed protein kinase genes under salt stress condition.**

Gene ID	Description	Length	E-value	Similarity (%)	Log ₂ fold change (PL6/PL1)				p-value	FDR
					0 h	3 h	12 h	24 h		
TraesCS1B02G098700	CBL-interacting protein kinase 17	466	0	89.58	5.64	1.70	4.46	1.42	3.76E-43	6.32E-41
TraesCS5B02G223900	CBL-interacting protein kinase 16	447	0	88.69	0.66	0.32	-0.20	-0.80	0.00187	0.011796
TraesCS4B02G319900	CBL-interacting protein kinase 9	443	0	94.32	1.37	0.71	0.36	0.35	4.87E-26	3.05E-24
TraesCS1B02G098600	CBL-interacting protein kinase 17	466	0	89.63	5.45	1.75	6.91	0.84	2.73E-25	1.65E-23
TraesCS5A02G492000	CBL-interacting protein kinase 9	446	0	94.25	0.72	0.47	0.04	0.28	8.66E-13	2.34E-11
TraesCS1D02G082500	CBL-interacting protein kinase 17	480	0	87.23	-0.21	0.29	-0.62	-0.89	3.29E-05	0.000341
TraesCS4D02G118500	CBL-interacting protein kinase 14	362	0	82.78	0.67	1.11	0.31	0.33	0.00488	0.026029
TraesCS1D02G082600	CBL-interacting protein kinase 17	448	0	86.72	0.36	0.01	-0.50	-0.37	6.13E-05	0.000598
TraesCS1A02G080600	CBL-interacting protein kinase 17	466	0	90.22	-0.39	-0.16	-0.76	-1.21	1.96E-07	0.000003
TraesCS1A02G080700	CBL-interacting protein kinase 17	471	0	89.6	-0.26	0.23	-0.86	-0.50	1.12E-10	2.52E-09
TraesCS4B02G120400	CBL-interacting protein kinase 14	444	0	92.95	-0.12	-0.80	0.86	0.38	0.000271	0.002245
TraesCS2D02G107100	CBL-interacting protein kinase 29	436	0	87.67	-0.24	-0.31	-0.51	0.08	0.005552	0.02886
TraesCS3B02G169300	CBL-interacting protein kinase 5	464	0	93.17	0.61	0.96	0.16	-0.54	4.65E-08	7.74E-07
TraesCS4D02G316500	CBL-interacting protein kinase 9	445	0	94.22	1.03	0.96	-0.10	0.27	3.23E-12	8.38E-11
TraesCS3D02G151500	CBL-interacting protein kinase 5	464	0	93.02	0.59	0.71	0.13	-0.26	2.39E-05	0.000254
TraesCS3A02G135500	CBL-interacting protein kinase 5	466	0	92.32	1.13	0.05	0.14	0.00	4.62E-06	5.69E-05
TraesCS1B02G104900	mitogen-activated protein kinase 14	549	0	92.96	3.98	1.64	3.09	1.98	6.05E-42	9.68E-40
TraesCS7A02G410700	mitogen-activated protein kinase 12	578	0	92.91	0.41	0.32	0.07	0.55	7.32E-06	8.69E-05

TraesCS5B02G075800	SNF1-type serine-threonine protein kinase	363	0	93.99	0.85	0.85	0.20	0.92	5.49E-05	0.000542
TraesCS5D02G081700	SNF1-type serine-threonine protein kinase	364	0	94.37	0.54	0.77	0.22	0.52	0.000294	0.002407
TraesCS1D02G308200	SNF1-related protein kinase regulatory subunit beta-1	280	0	82.88	-1.25	-0.65	0.17	0.67	7.37E-05	0.000706
TraesCS5A02G069500	SNF1-type serine-threonine protein kinase	360	0	95.18	-0.78	-0.29	-0.35	0.67	0.002772	0.01638

3 Bold numbers indicate more than two-fold changes in expression.

Table 3 (on next page)

Table 3. List of differentially expressed salt stress responsive genes selected by MapMan program

1 **Table 3:**2 **List of differentially expressed salts stress responsive genes selected by MapMan program.**

Gene ID	Description	Length	E-value	Similarity (%)	Log ₂ fold change (PL6/PL1)				p-value	FDR	BinName from MapMan
					0 h	3 h	12 h	24 h			
TraesCSU02G196100	Pseudo-response regulator (PRR)	660	0	97.11	-0.67	-0.01	-0.99	-4.44	4.11E-07	5.98E-06	Circadian clock system
TraesCS5D02G078500	Kinesin-like protein KIN-12F isoform X2	3015	0	84.6	-0.73	-0.21	-0.05	-2.42	7.62E-15	2.4E-13	Cytoskeleton organization
TraesCS1B02G123200	Kinesin-like protein KIN-13A	519	0	92.31	5.27	2.00	5.67	2.61	1.73E-62	8.72E-60	Cytoskeleton organization
TraesCS1B02G024500	Actin-7	377	0	99.58	4.70	4.81	5.63	2.86	4.55E-63	2.37E-60	Cytoskeleton organization
TraesCS5B02G491800	Actin depolymerization factor-like protein	147	6.3E-104	88.78	0.86	-0.12	0.73	-2.31	1.92E-05	0.00021	Cytoskeleton organization
TraesCS5D02G492300	Actin depolymerization factor-like protein	147	6.3E-105	87.63	0.55	0.09	0.38	-3.25	2.08E-11	5.07E-10	Cytoskeleton organization
TraesCS1B02G069300	Protein unc-13 homolog	1107	0	93.26	9.87	9.73	10.07	1.73	1.97E-53	5.97E-51	Cell wall organization
TraesCS6D02G048900	Melibiose family protein	637	0	80.94	-2.04	-3.80	-2.48	-0.04	0.000177	0.001532	Cell wall organization
TraesCS1B02G084600	Hydroxyproline O-galactosyltransferase GALT3	591	0	83.91	3.76	2.71	2.78	0.79	5.51E-16	1.89E-14	Cell wall organization
TraesCS1D02G019000	Tricin synthase 1	248	1.8E-180	79.05	-1.48	0.37	-2.29	-0.17	6.39E-09	1.18E-07	Cell wall organization
TraesCS5D02G488900	Caffeic acid O-methyltransferase	353	0	86.01	-1.86	-2.56	-4.53	0.63	7.23E-20	3.17E-18	Cell wall organization

TraesCS1B02G098800	Acyl transferase 4	435	0	80.27	8.49	2.00	8.69	2.57	4.28E-31	3.63E-29	Cell wall organization
TraesCS3D02G116600	Alkane hydroxylase MAH1-like	517	0	88.56	0.02	0.08	-2.60	-2.99	0.001075	0.00741	Cell wall organization
TraesCS5D02G127300	Aldehyde dehydrogenase family 3 member H1-like	479	0	86.99	0.49	-0.29	-2.17	-1.78	2.63E-10	5.72E-09	Cell wall organization
TraesCS2A02G045800	GDSL esterase/lipase LTL1	369	0	90.05	9.20	1.62	8.58	8.50	3.69E-36	4.22E-34	Cell wall organization

3 Bold numbers indicate more than two-fold changes in expression.